Modeling Sea Ice as a Multiscale Composite Material

Kenneth M. Golden
Department of Mathematics
University of Utah

ONR Program Review
15 July 2020

Beaufort Sea
Golden

SEA ICE covers ~12% of Earth's ocean surface

- boundary between ocean and atmosphere
- mediates exchange of heat, gases, momentum
- global ocean circulation
- hosts rich ecosystem
- indicator of climate change

Sea Ice is a Multiscale Composite Material

MICROSCALE

brine inclusions

Weeks & Assur 1969

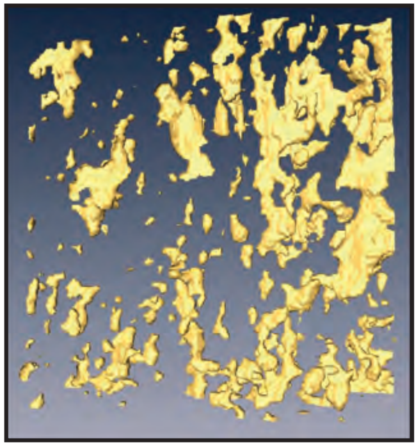

H. Eicken

Golden *et al. GRL* 2007

polycrystals

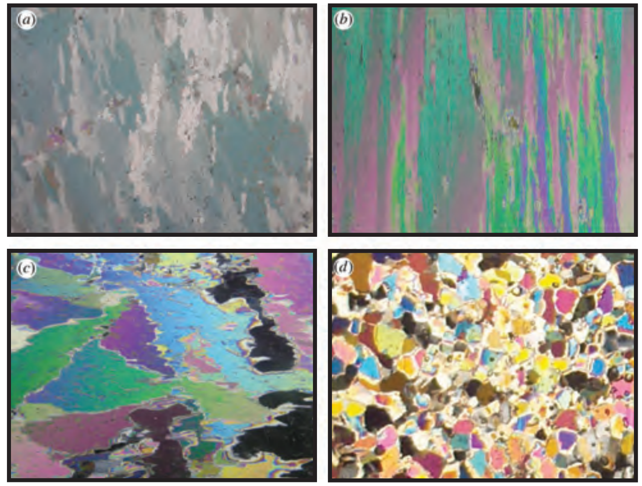

Gully *et al. Proc. Roy. Soc. A* 2015

brine channels

D. Cole

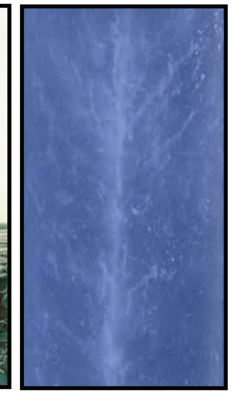

K. Golden

millimeters **centimeters**

MESOSCALE

Arctic melt ponds

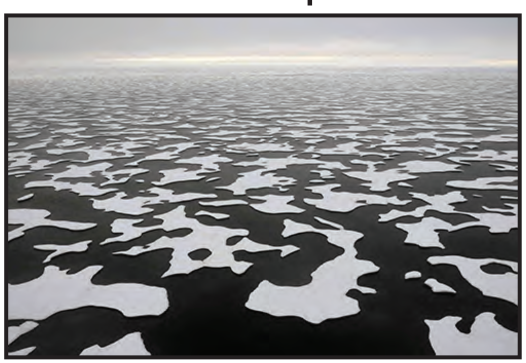

K. Frey

pressure ridges

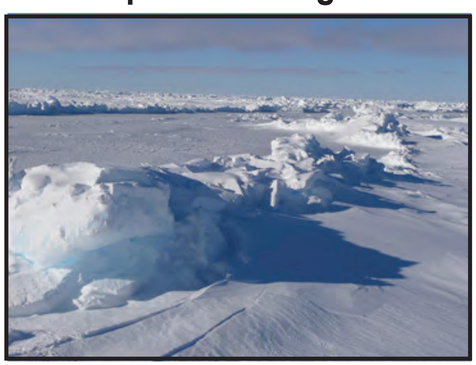

K. Golden

meters

MACROSCALE

sea ice floes

J. Weller

sea ice pack

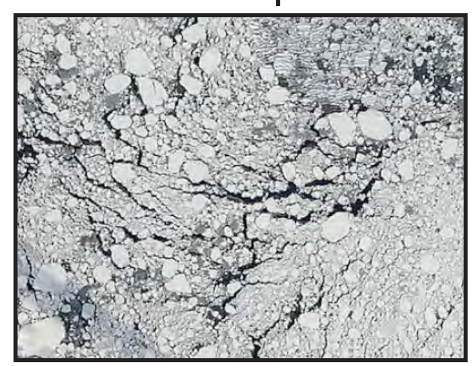

NASA

kilometers

HOMOGENIZATION for Composite Materials

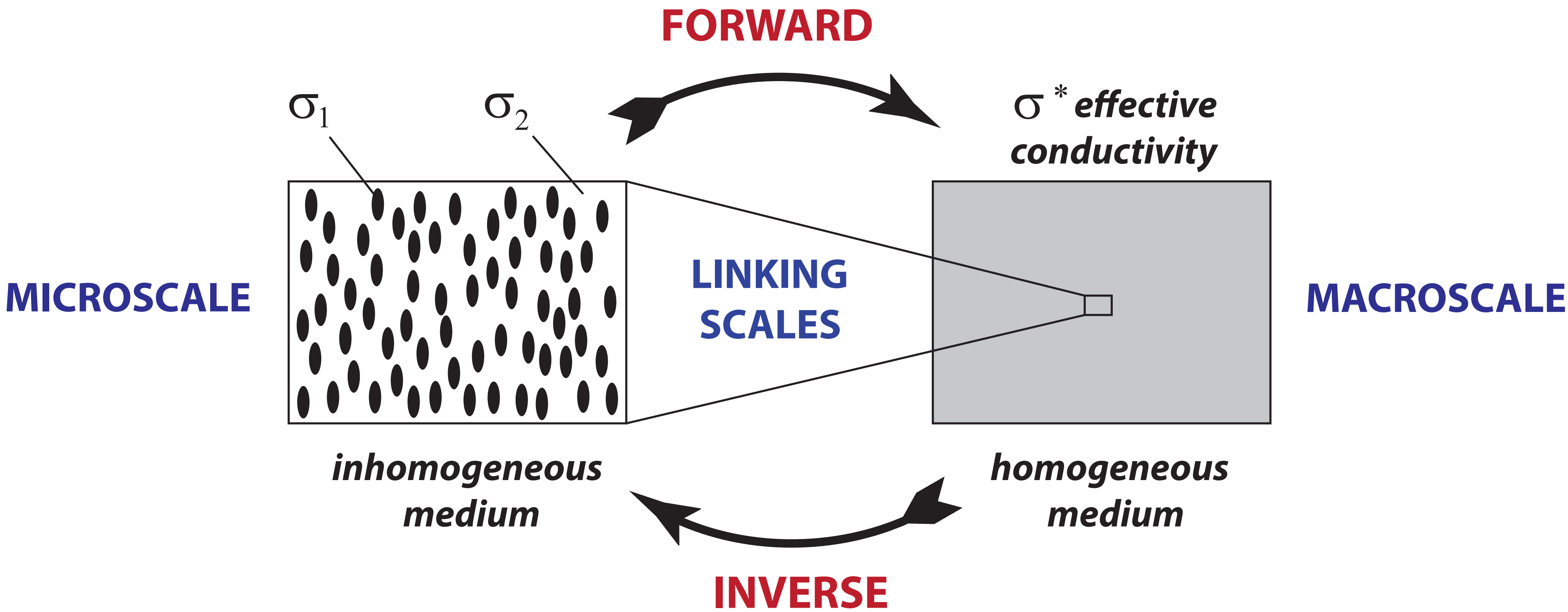

Maxwell 1873 : effective conductivity of a dilute suspension of spheres
Einstein 1906 : effective viscosity of a dilute suspension of rigid spheres in a fluid

*Wiener 1912 : arithmetic and harmonic mean **bounds** on effective conductivity*
*Hashin and Shtrikman 1962 : variational **bounds** on effective conductivity*

widespread use of composites in late 20th century due in large part to advances in mathematically predicting their effective properties

What is this talk about? homogenization for multiscale composites

the role of "microstructure" in determining sea ice effective properties

Using methods of **homogenization and statistical physics** to LINK SCALES in the sea ice system ... compute effective behavior on scales relevant to coarse-grained sea ice and climate models, process studies, ...

MICROSCALE: brine + polycrystalline structure; EM and fluid transport

MESOSCALE: advection diffusion, thermal transport, waves, melt ponds

MACROSCALE: ice transport, MIZ width and location, low order models

A tour of Stieltjes integrals in the study of sea ice and its role in climate.

Solving problems in physics of sea ice drives advances in theory of composite materials.

cross - pollination

bone, stealthy coatings
magnets, rat brains, RMT

How do scales interact in the sea ice system?

NASA

basin scale - grid scale albedo

Linking Scales

km scale melt ponds

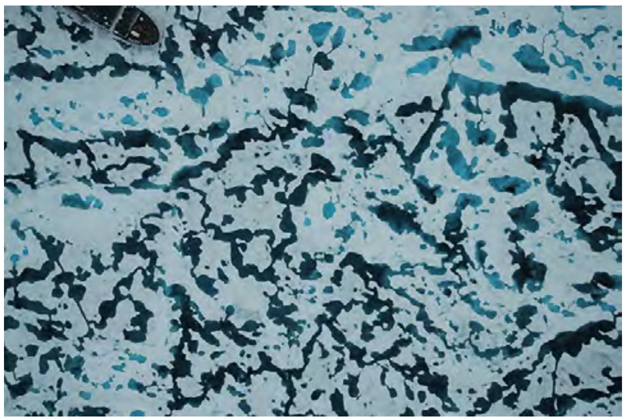

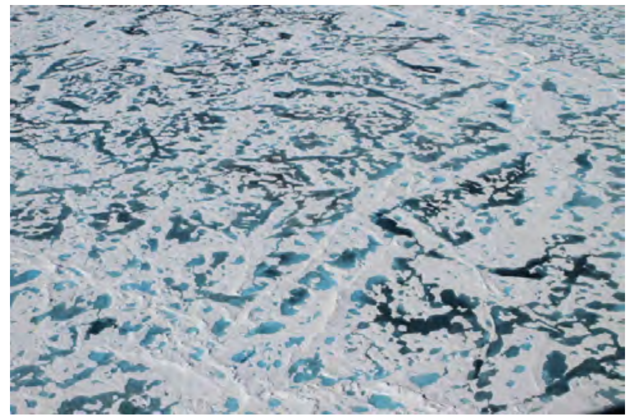

km scale melt ponds

Perovich

Linking Scales

mm scale brine inclusions

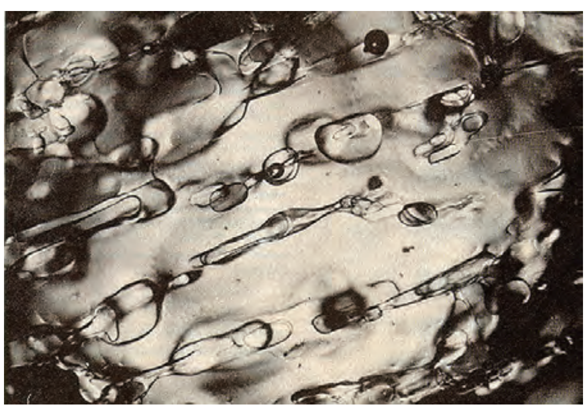

meter scale snow topography

microscale

Critical behavior of fluid transport in sea ice

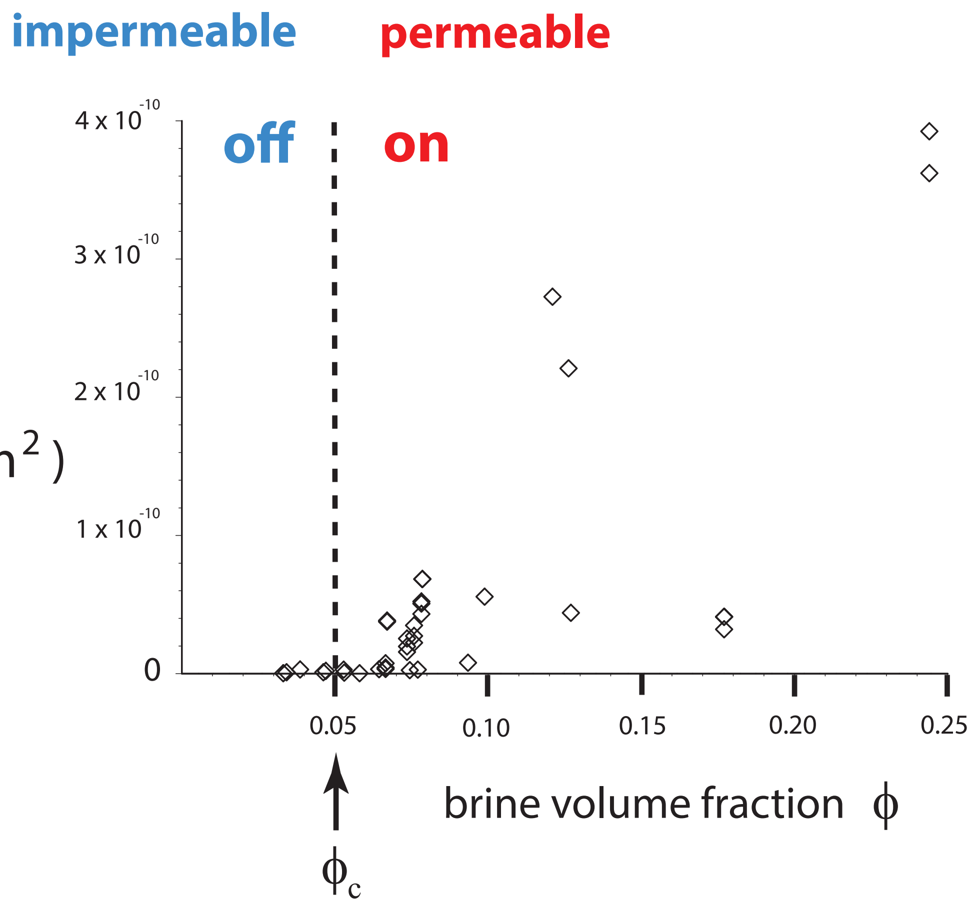

Arctic field data

vertical fluid permeability k (m^2)

"on - off" switch for fluid flow

critical brine volume fraction $\phi_c \approx 5\% \longleftrightarrow T_c \approx -5^\circ C,\ S \approx 5$ ppt

RULE OF FIVES

Golden, Ackley, Lytle Science 1998
Golden, Eicken, Heaton, Miner, Pringle, Zhu GRL 2007
Pringle, Miner, Eicken, Golden J. Geophys. Res. 2009

brine volume fraction and ***connectivity*** increase with temperature

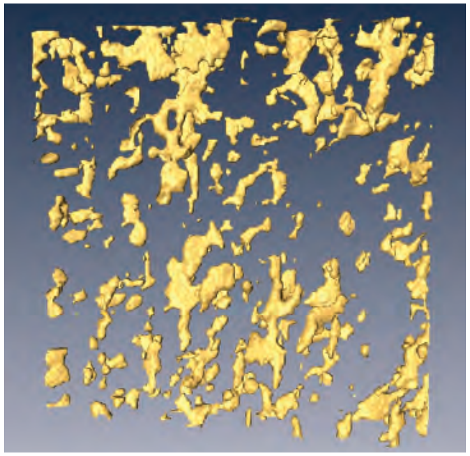

T = -15 °C, $\phi = 0.033$

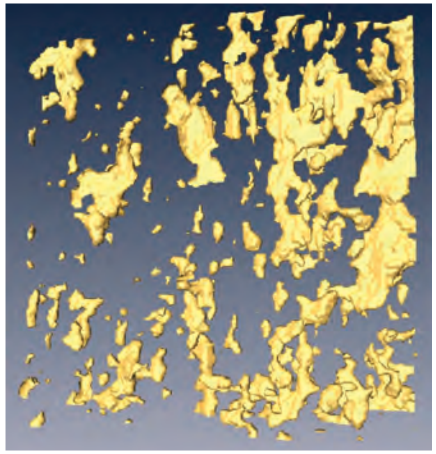

T = -6 °C, $\phi = 0.075$

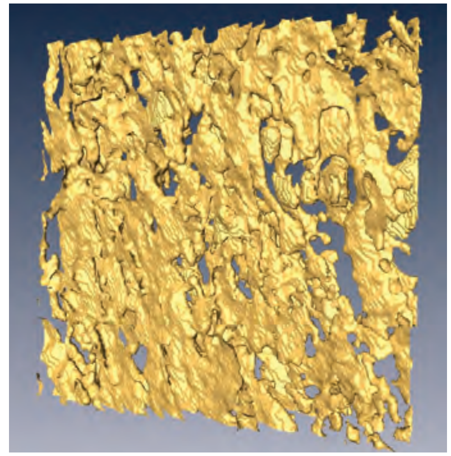

T = -3 °C, $\phi = 0.143$

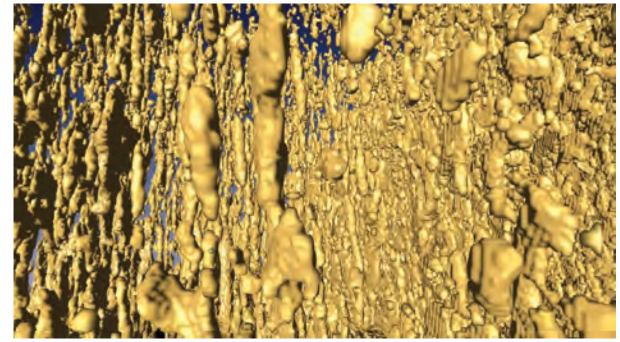

T = -4 °C, $\phi = 0.113$

X-ray tomography for brine phase in sea ice

Golden, Eicken, *et al., Geophysical Research Letters* 2007

PERCOLATION THRESHOLD $\phi_c \approx 5\ \%$

Golden, Ackley, Lytle, *Science* 1998

impermeable

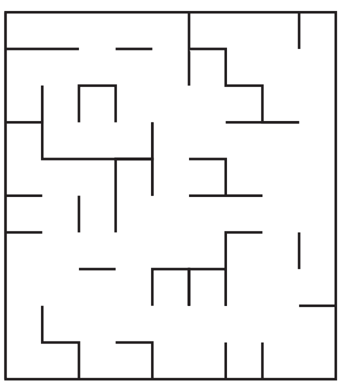

$p = 1/3$

permeable

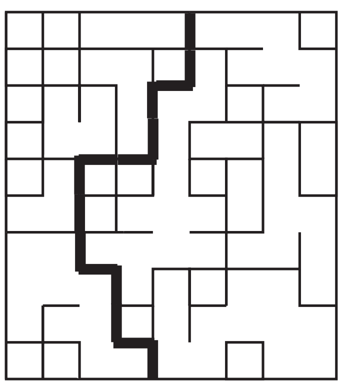

$p = 2/3$

lattice percolation

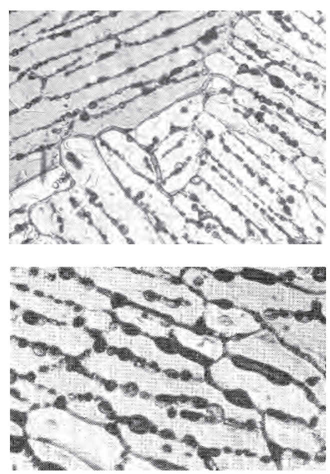

sea ice

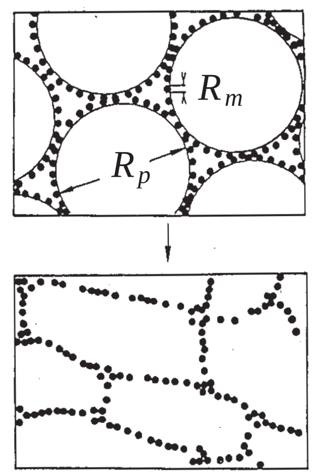

compressed powder

Kusy, Turner
Nature 1971

stealth

continuum percolation

Thermal evolution of permeability and microstructure in sea ice

Golden, Eicken, Heaton, Miner, Pringle, Zhu, Geophysical Research Letters 2007

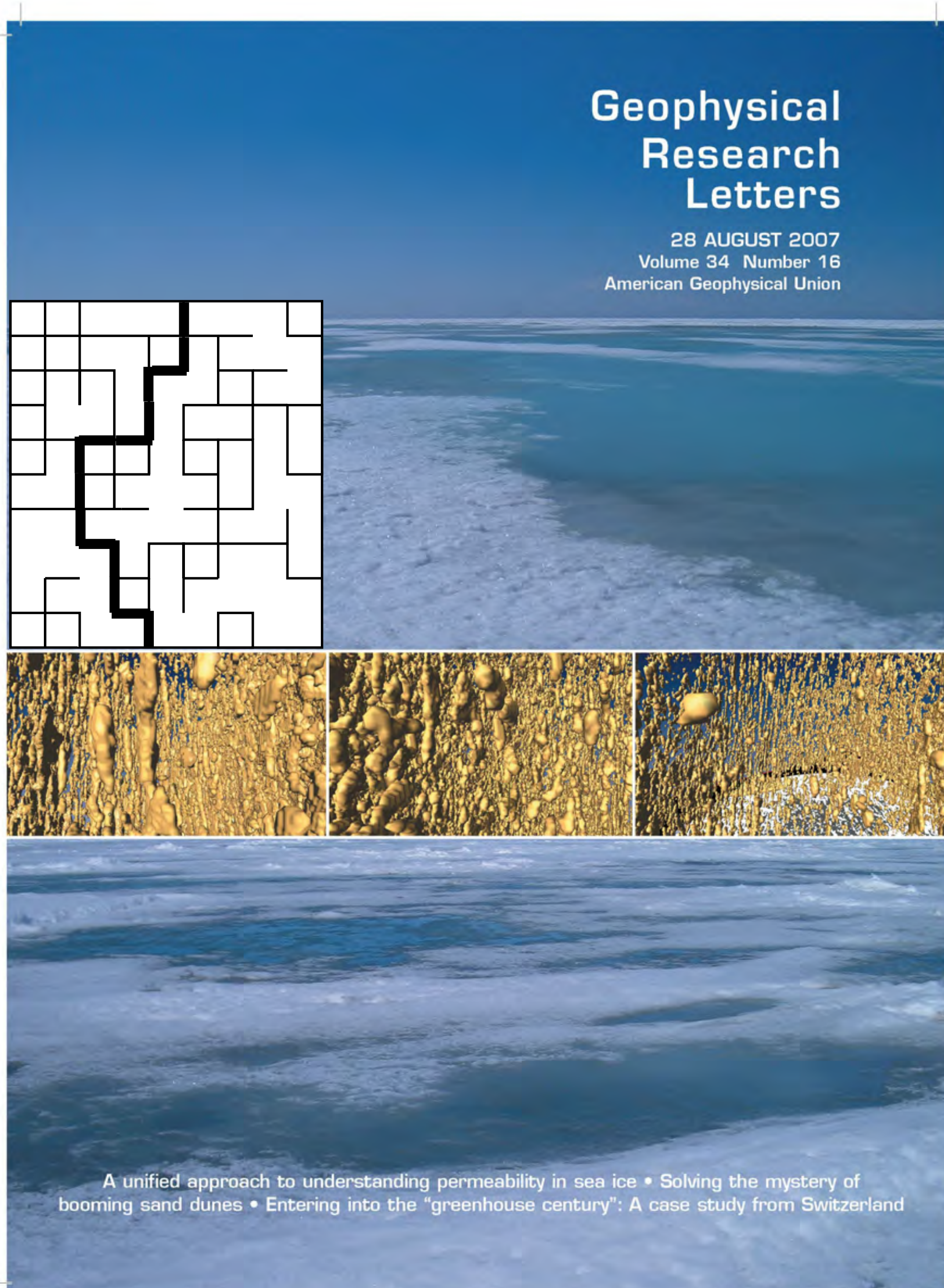

micro-scale

controls

macro-scale

processes

percolation theory

$$k(\phi) = k_0 (\phi - 0.05)^2$$

critical exponent

t

$$k_0 = 3 \times 10^{-8} \text{ m}^2$$

hierarchical model
network model
rigorous bounds

agree closely with
field data

X-ray tomography for brine inclusions

unprecedented look at thermal evolution of brine phase and its connectivity

confirms rule of fives

Pringle, Miner, Eicken, Golden
J. Geophys. Res. 2009

Sea ice algae secrete extracellular polymeric substances (EPS) affecting evolution of brine microstructure.

How does EPS affect fluid transport? **How does the biology affect the physics?**

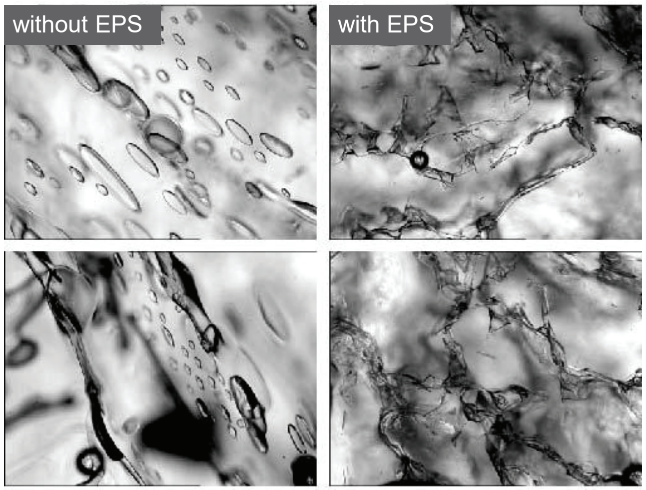

Krembs, Eicken, Deming, PNAS 2011

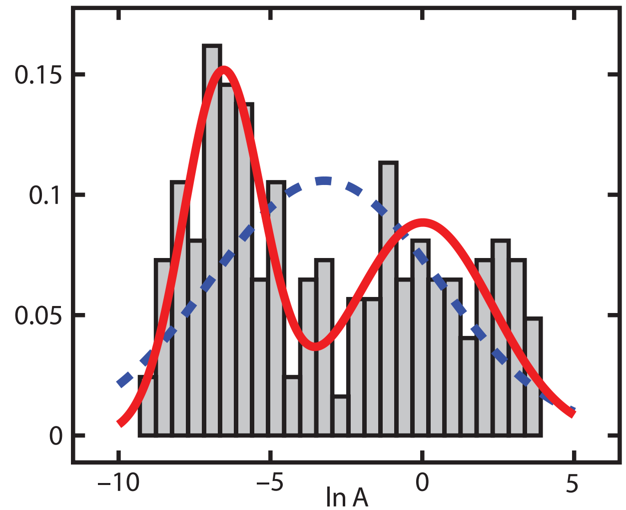

RANDOM PIPE MODEL

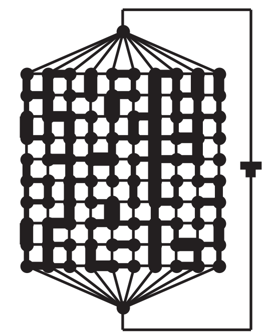

- 2D random pipe model with bimodal distribution of pore sizes
- **Rigorous bound on permeability *k*; results predict observed drop in *k***

Steffen, Epshteyn, Zhu, Bowler, Deming, Golden
***Multiscale Modeling and Simulation*, 2018**

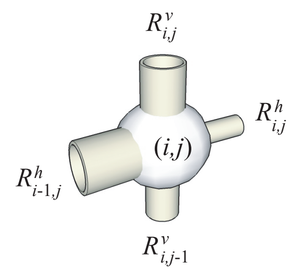

3D extension, effect of EPS clogging, blockage

Anna Hyde, Jingyi Zhu, Ken Golden

Zhu, Jabini, Golden, Eicken, Morris
***Ann. Glac.* 2006**

The Melt Pond Conundrum:

How can ponds form on top of sea ice that is highly permeable?

C. Polashenski, K. M. Golden, D. K. Perovich, E. Skyllingstad, A. Arnsten, C. Stwertka, N. Wright

Percolation Blockage: A Process that Enables Melt Pond Formation on First Year Arctic Sea Ice

J. Geophys. Res. Oceans 2017

2014 Study of Under Ice Blooms in the Chuckchi Ecosystem (SUBICE) aboard USCGC Healy

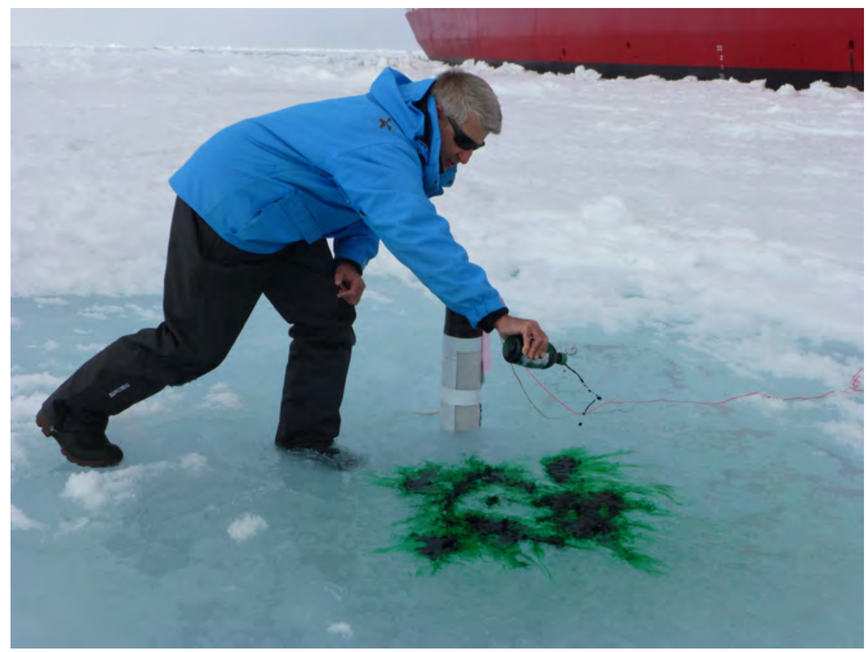

higher threshold for fluid flow in granular sea ice

microscale details impact "mesoscale" processes

nutrient fluxes for microbes
melt pond drainage
snow-ice formation

columnar

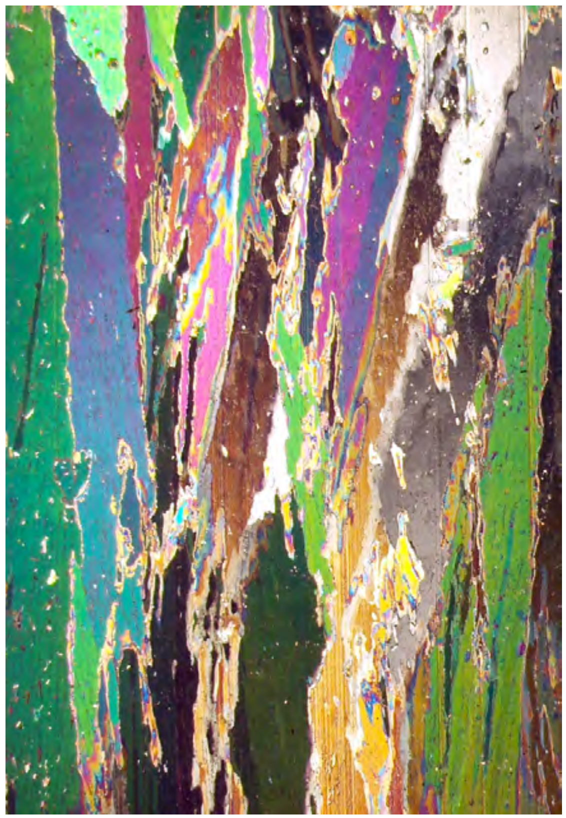

5%

granular

10%

Golden, Sampson, Gully, Lubbers, Tison 2020

electromagnetically distinguishing ice types

Kitsel Lusted, Elena Cherkaev, Ken Golden

Remote sensing of sea ice

sea ice thickness
ice concentration

INVERSE PROBLEM

Recover sea ice properties from electromagnetic (EM) data

ε^*

effective complex permittivity (dielectric constant, conductivity)

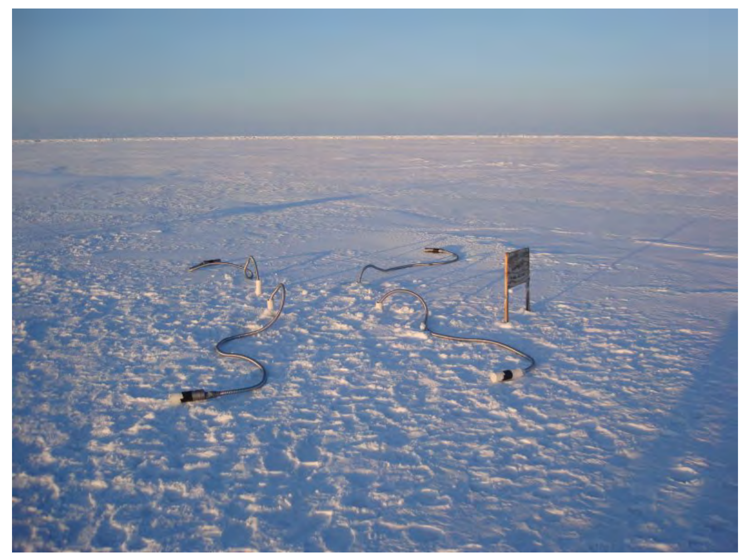

brine volume fraction
brine inclusion connectivity

Effective complex permittivity of a two phase composite in the quasistatic (long wavelength) limit

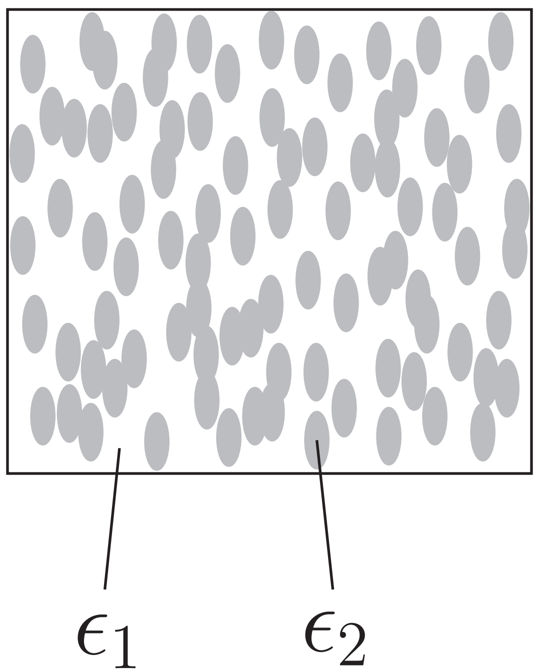

$$\Big\} \; \epsilon^*$$

$$D = \epsilon E$$

$$\nabla \cdot D = 0$$

$$\nabla \times E = 0$$

$$\langle D \rangle = \epsilon^* \langle E \rangle$$

p_1 , p_2 = volume fractions of the components

$$\epsilon^* = \epsilon^* \left(\frac{\epsilon_1}{\epsilon_2} \, , \text{ composite geometry} \right)$$

What are the effective propagation characteristics of an EM wave (radar, microwaves) in the medium?

Analytic Continuation Method for Homogenization

Bergman (1978), Milton (1979), Golden and Papanicolaou (1983), Theory of Composites, Milton (2002)

Stieltjes integral representation for homogenized parameter

separates geometry from parameters

geometry

$$F(s) = 1 - \frac{\epsilon^*}{\epsilon_2} = \int_0^1 \frac{d\mu(z)}{s - z} \qquad s = \frac{1}{1 - \epsilon_1/\epsilon_2}$$

material parameters

μ

- spectral measure of self adjoint operator $\Gamma\chi$
- mass $= p_1$
- higher moments depend on n-point correlations

$$\Gamma = \nabla(-\Delta)^{-1}\nabla\cdot$$

$\chi =$ characteristic function of the brine phase

resolvent

$$E = s\,(s + \Gamma\chi)^{-1} e_k$$

$\Gamma\chi$: microscale $\rightarrow$ macroscale

$\Gamma\chi$ *links scales*

Golden and Papanicolaou, Comm. Math. Phys. 1983

forward and inverse bounds on the complex permittivity of sea ice

forward bounds

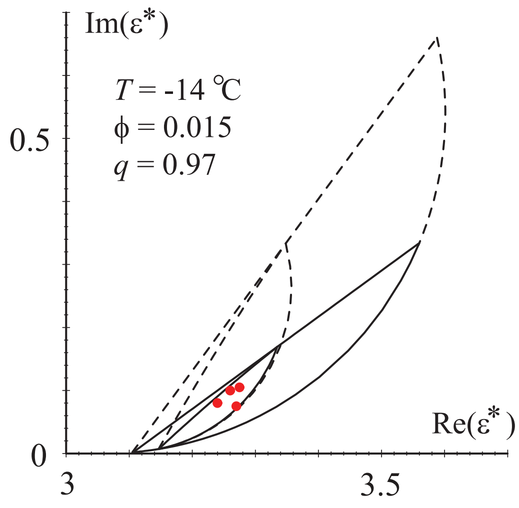

4.75 GHz data

matrix particle

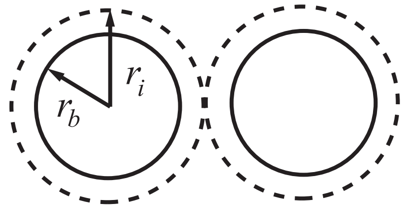

$$q = r_b / r_i$$

$$0 < q < 1$$

Golden 1995, 1997

inverse bounds

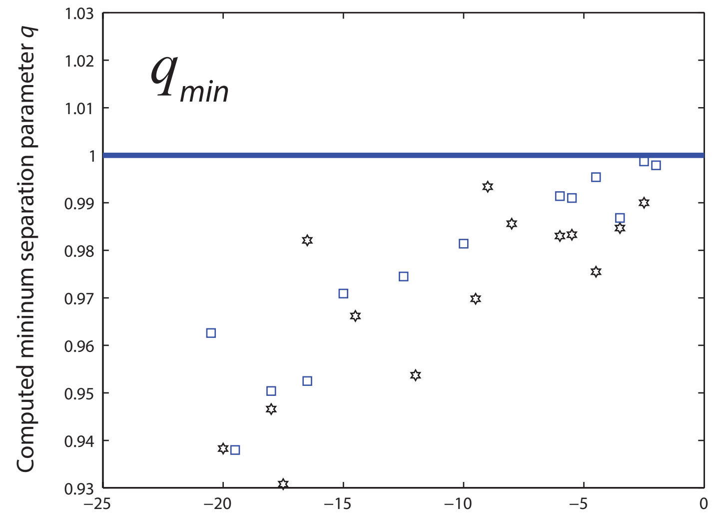

Slab temperature °C

Inverse Homogenization

Cherkaev and Golden (1998), Day and Thorpe (1999), Cherkaev (2001), McPhedran, McKenzie, Milton (1982), *Theory of Composites*, Milton (2002)

ε^* → ***composite geometry*** **(spectral measure μ)**

inverse bounds and recovery of brine porosity

Gully, Backstrom, Eicken, Golden
Physica B, 2007

inversion for brine inclusion separations in sea ice from measurements of effective complex permittivity ε^*

rigorous inverse bound on spectral gap

construct algebraic curves which bound admissible region in (p,q)-space

Orum, Cherkaev, Golden
Proc. Roy. Soc. A, 2012

direct calculation of spectral measures

Murphy, Hohenegger, Cherkaev, Golden, *Comm. Math. Sci.* 2015

- depends only on the composite geometry
- discretization of microstructural image gives binary network
- fundamental operator becomes a random matrix
- spectral measure computed from eigenvalues and eigenvectors

once we have the spectral measure μ it can be used in Stieltjes integrals for other transport coefficients:

electrical and thermal conductivity, complex permittivity, magnetic permeability, diffusion, fluid flow properties

earlier studies of spectral measures

Day and Thorpe 1996
Helsing, McPhedran, Milton 2011

Spectral computations for sea ice floe configurations

spectral measures

eigenvalue spacing distributions

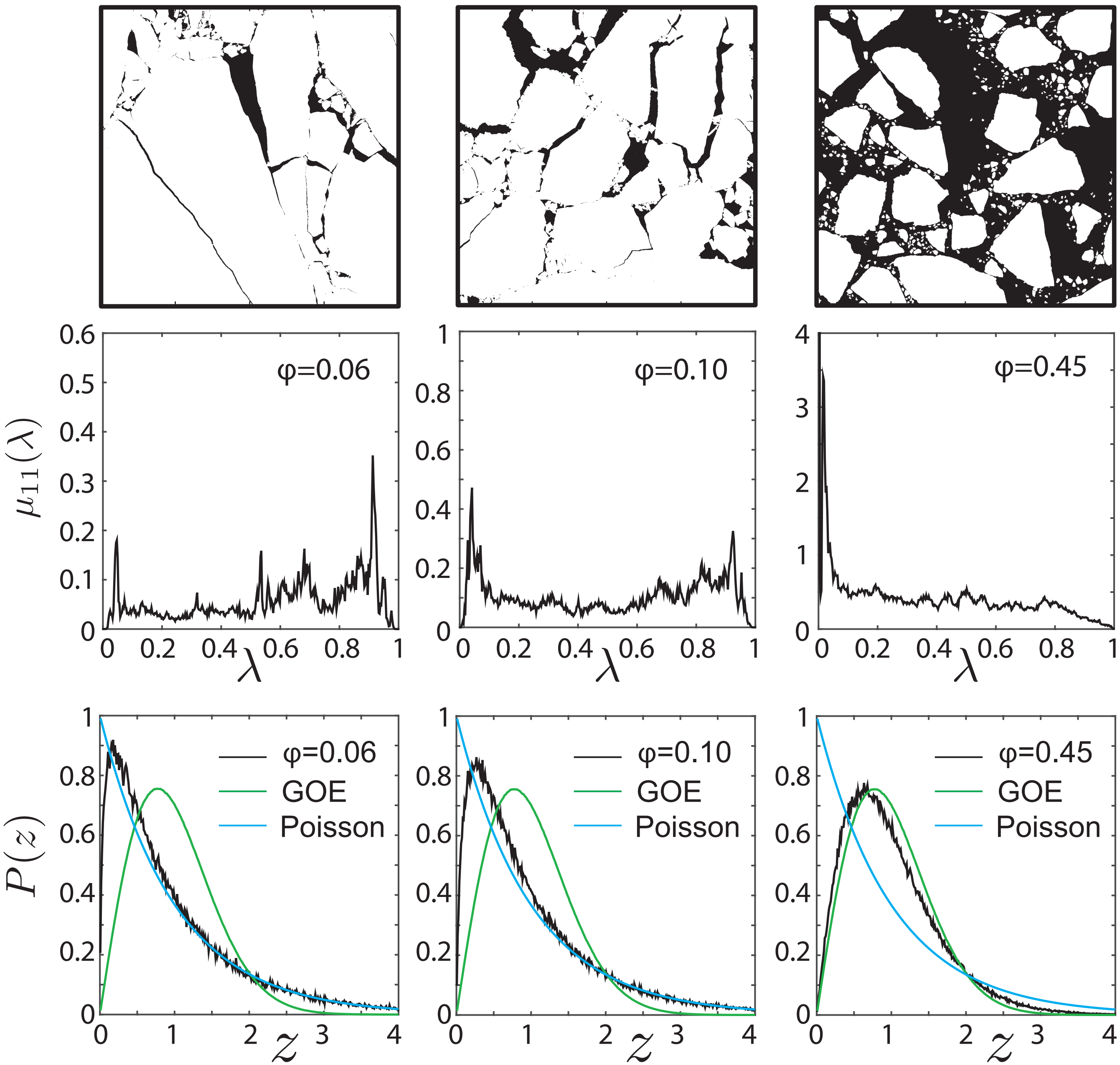

UNIVERSAL *Wigner-Dyson distribution*

uncorrelated → **level repulsion**

ANDERSON TRANSITION

Murphy, Cherkaev, Golden
***Phys. Rev. Lett.* 2017**

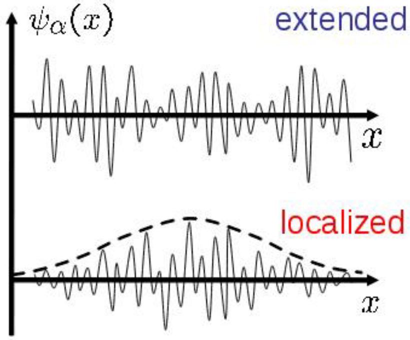

metal / insulator transition

localization

Anderson 1958
Mott 1949
Shklovshii et al 1993
Evangelou 1992

Anderson transition in wave physics:
quantum, optics, acoustics, water waves, ...

from analysis of spectral measures for brine, melt ponds, ice floes

we find percolation-driven

Anderson transition for classical transport in composites

mobility edges, localization transition, universal spectral statistics

Murphy, Cherkaev, Golden Phys. Rev. Lett. 2017

Order to disorder in quasiperiodic materials

Morison, Murphy, Cherkaev, Golden 2020

Parameterized Moiré Pattern Creates Tunable Microgeometry

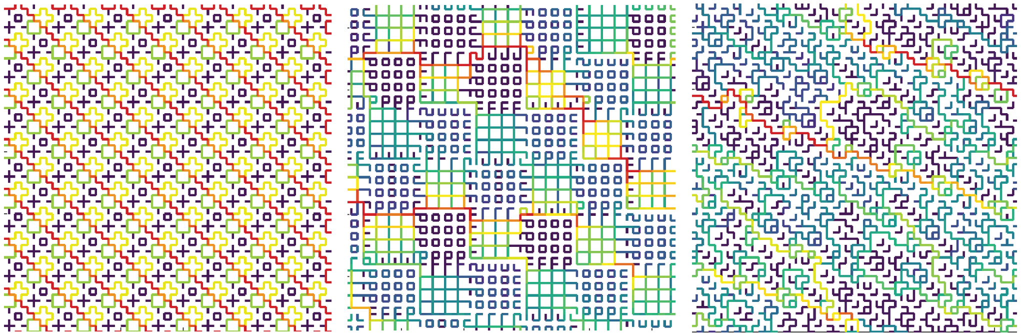

Anderson transition as QP is tuned

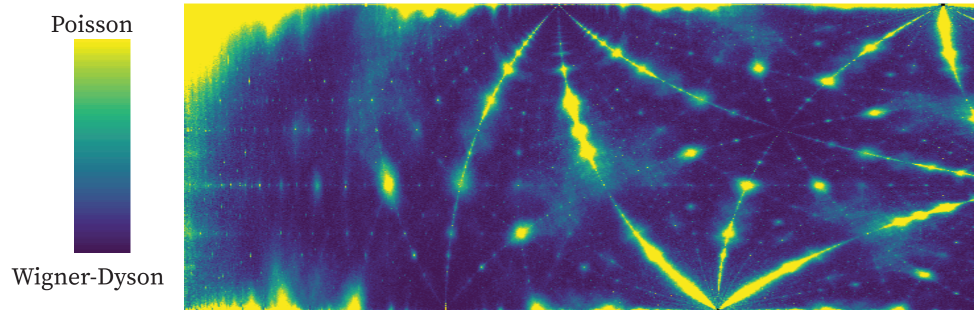

Bounds on the complex permittivity of polycrystalline materials by analytic continuation

Adam Gully, Joyce Lin,
Elena Cherkaev, Ken Golden

- **Stieltjes integral representation for effective complex permittivity**

  Milton (1981, 2002), Barabash and Stroud (1999), ...

- **Forward and inverse bounds**

  orientation statistics

- **Applied to sea ice using two-scale homogenization**

- **Inverse bounds give method for distinguishing ice types using remote sensing techniques**

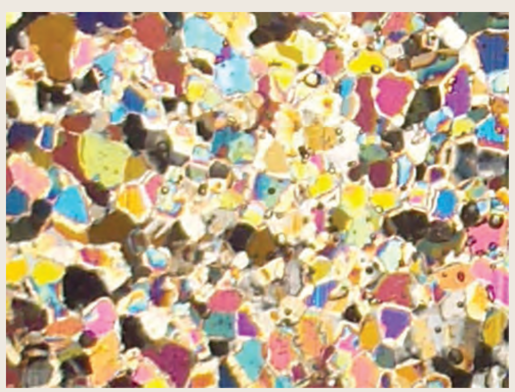

Proc. Roy. Soc. A 8 Feb 2015

21/01/15 1:47 PM

two scale homogenization for polycrystalline sea ice

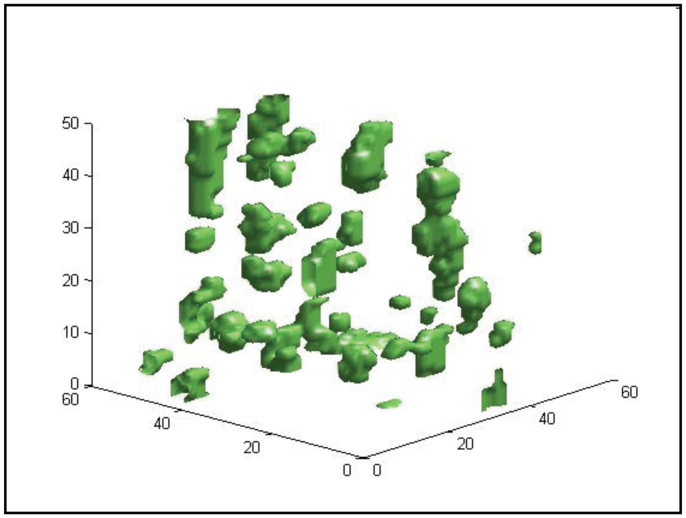

numerical homogenization for single crystal

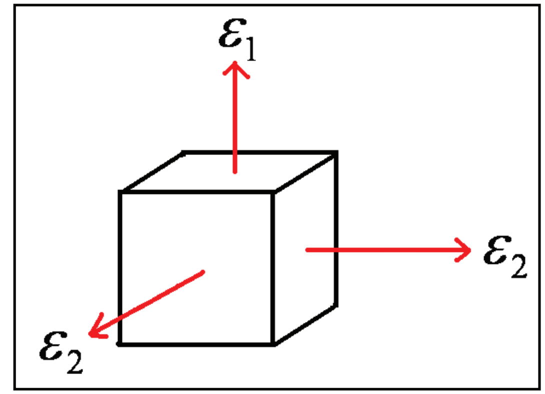

analytic continuation for polycrystals

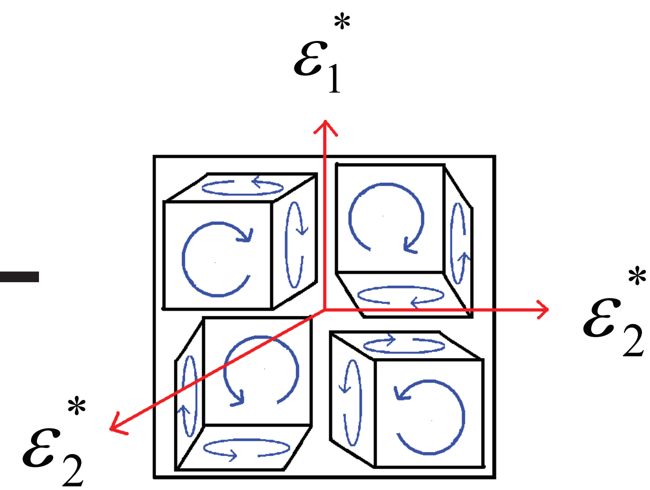

bounds

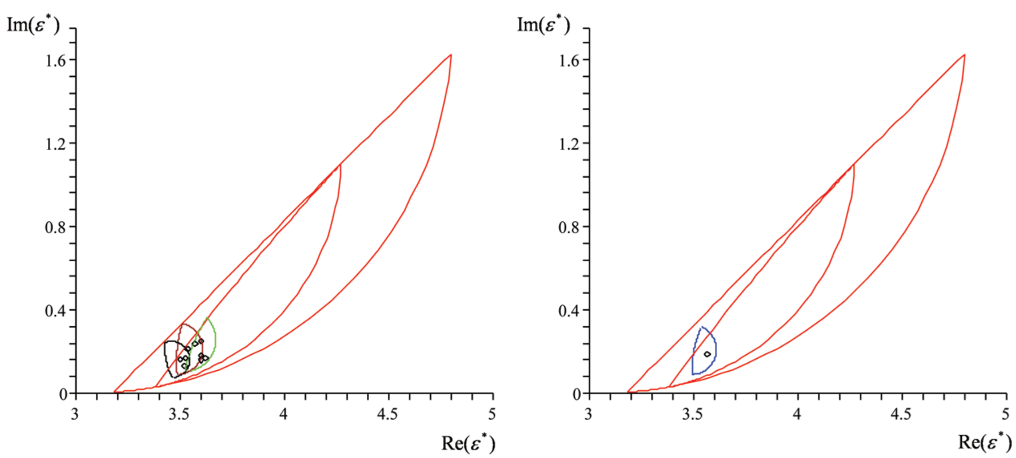

Gully, Lin, Cherkaev, Golden, Proc. Roy. Soc. A (and cover) 2015

Rigorous bounds on the complex permittivity tensor of sea ice with polycrystalline anisotropy within the horizontal plane

Kenzie McLean, Elena Cherkaev, Ken Golden 2020

motivated by Weeks and Gow, *JGR* 1979: c-axis alignment in Arctic fast ice off Barrow

Golden and Ackley, *JGR* 1981: radar propagation model in aligned sea ice

input: orientation statistics

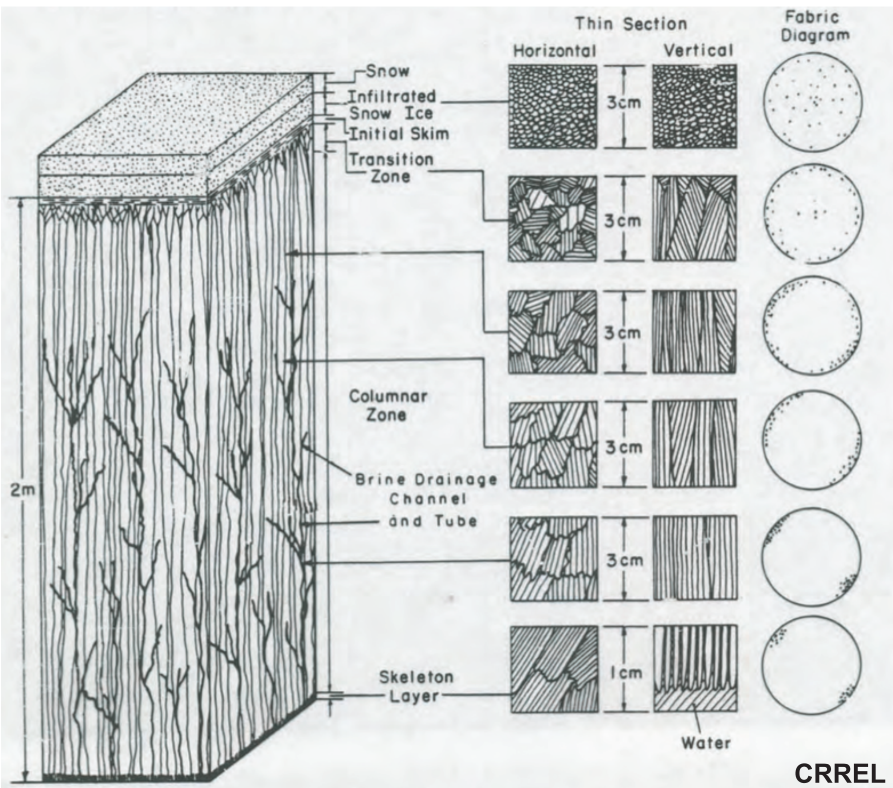

output: bounds

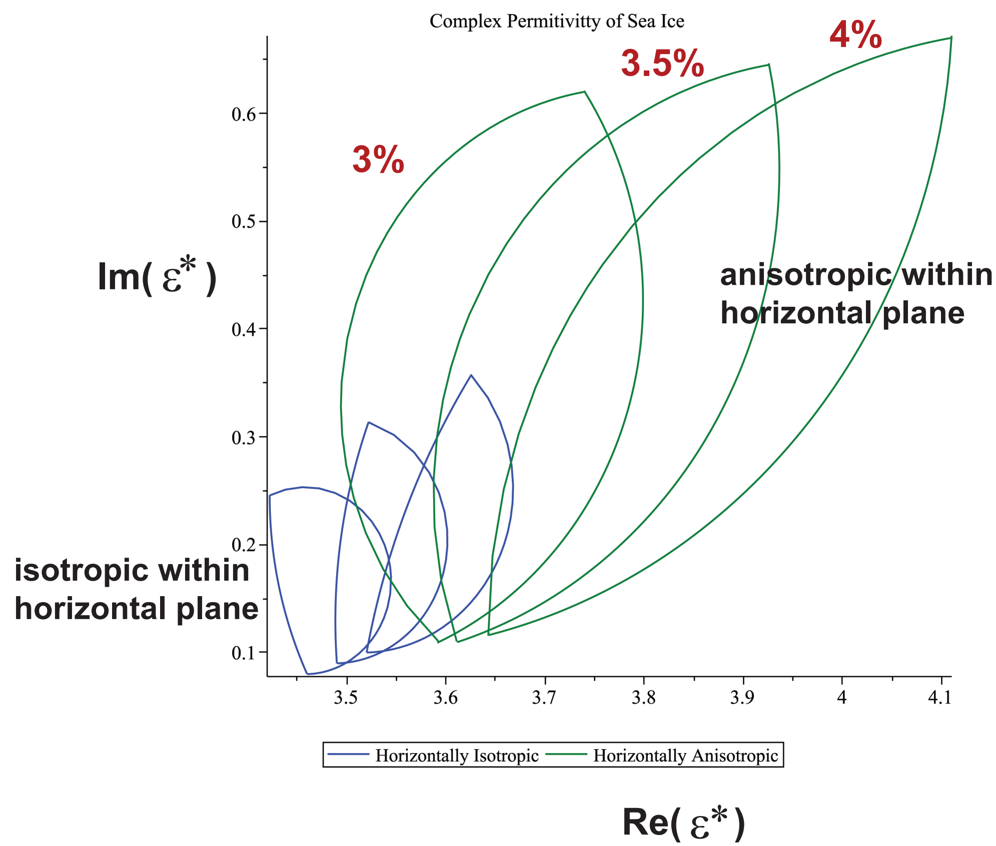

mesoscale

wave propagation in the marginal ice zone

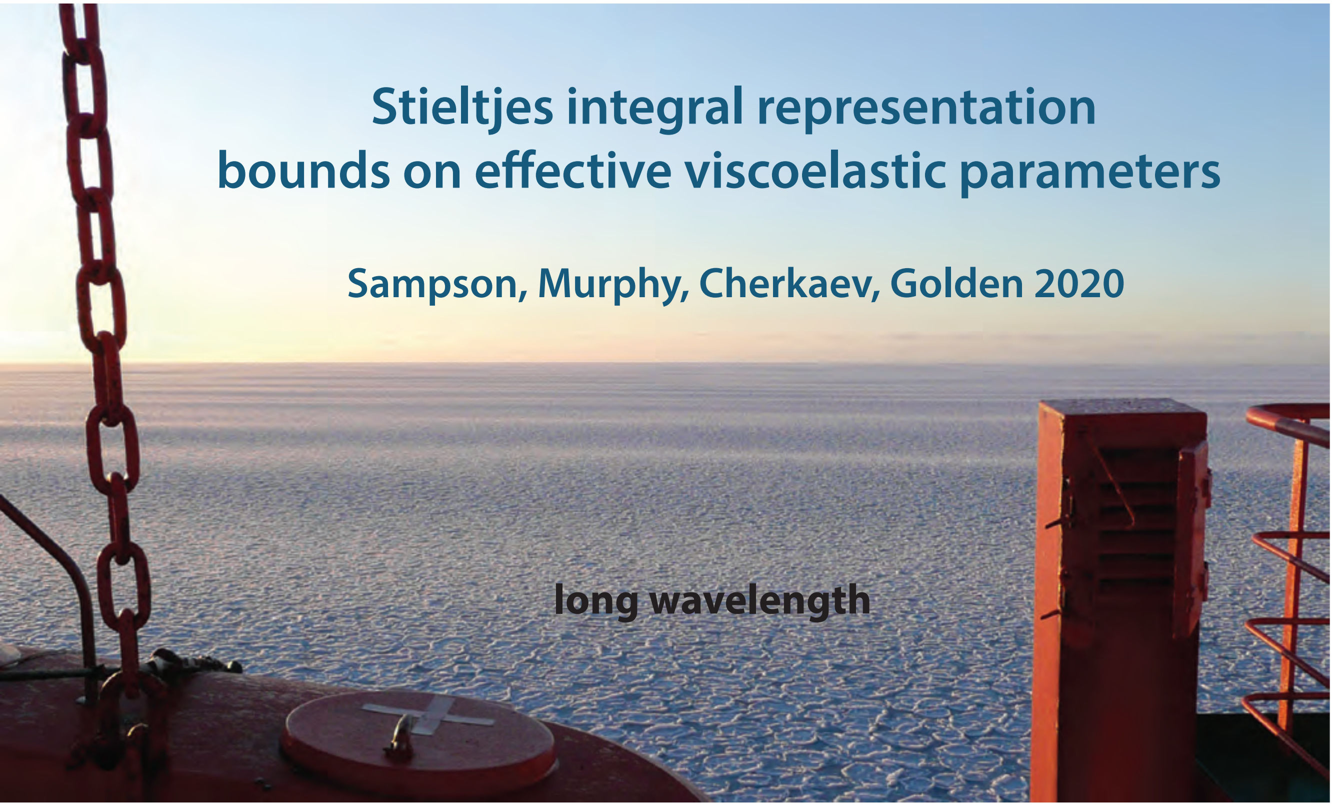

Stieltjes integral representation
bounds on effective viscoelastic parameters

Sampson, Murphy, Cherkaev, Golden 2020

long wavelength

$$\langle \sigma_{ij} \rangle = C^*_{ijkl} \langle \epsilon_{kl} \rangle$$

ϵ_0 **avg strain**

$$C^*_{ijkl} = \nu^* \left(\delta_{ik}\delta_{jl} + \delta_{il}\delta_{jk} - \frac{2}{3}\delta_{ij}\delta_{kl} \right) = \nu^* \lambda_s$$

$$F(s) = 1 - \frac{\nu^*}{\nu_2} \qquad s = \frac{1}{1 - \frac{\nu_1}{\nu_2}}$$

$$F(s) = ||\epsilon_0||^{-2} \int_\Sigma \frac{d\mu(\lambda)}{s - \lambda}$$

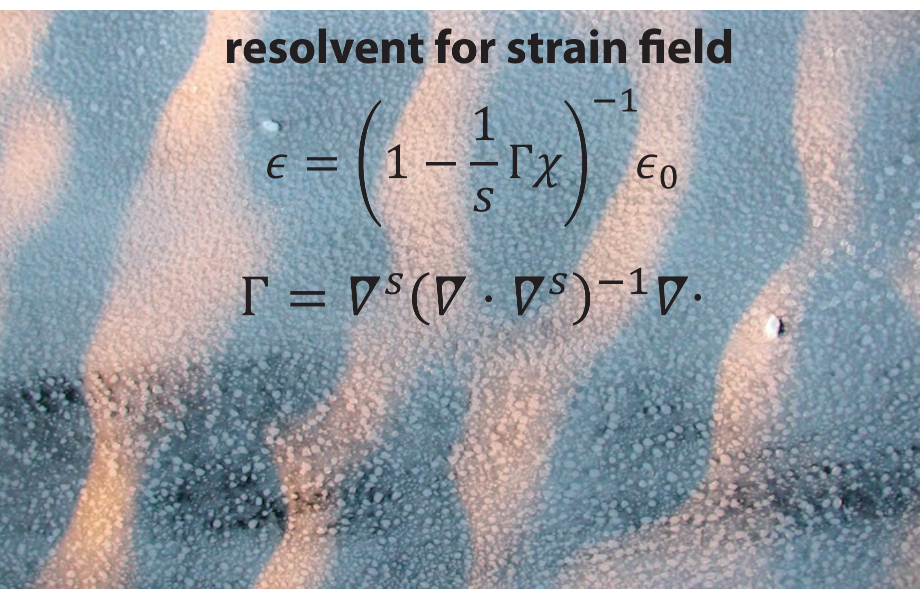

resolvent for strain field

$$\epsilon = \left(1 - \frac{1}{s} \Gamma \chi \right)^{-1} \epsilon_0$$

$$\Gamma = \nabla^s (\nabla \cdot \nabla^s)^{-1} \nabla \cdot$$

local

$$\sigma_{ij} = C_{ijkl} \epsilon_{kl}$$

quasistatic

$$\nabla \cdot \sigma = 0$$

bounds on the effective complex viscoelasticity

complex elementary bounds
(fixed area fraction of floes)

$\nu_1 = 10^7 + i\,4875$ **pancake ice**

$\nu_2 = 5 + i\,0.0975$ **slush / frazil**

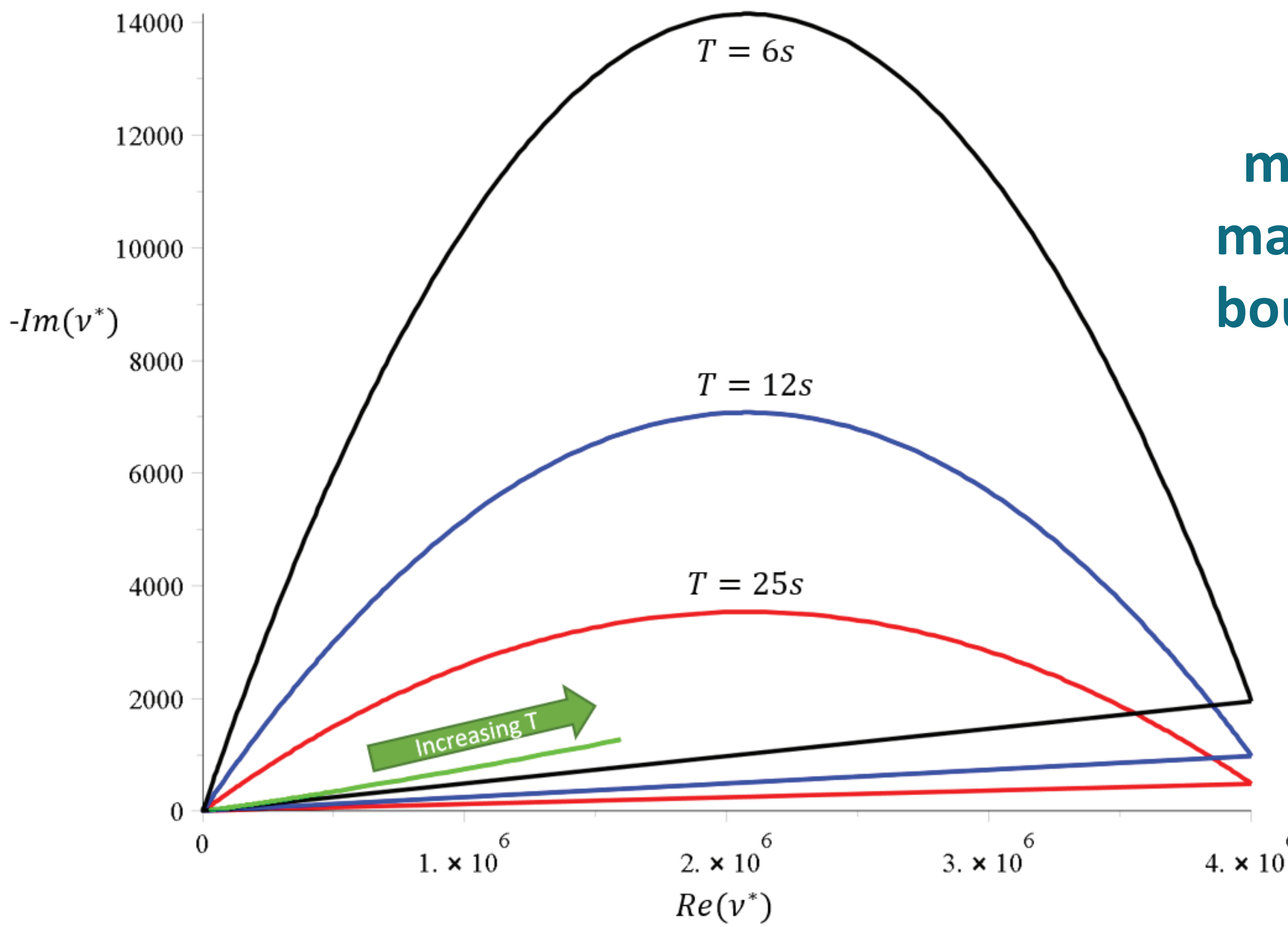

+
much tighter matrix particle bounds + data

Sampson, Murphy, Cherkaev, Golden 2020

1D Model of Ocean Surface Wave Attenuation in Sea Ice

David Morison, Samir Suthar, Elena Cherkaev, Ken Golden

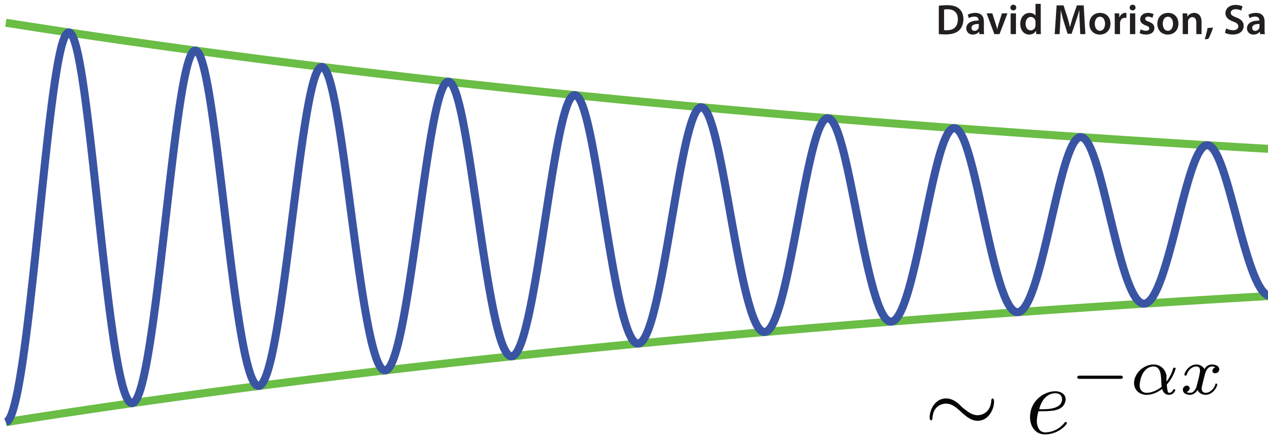

$$\sim e^{-\alpha x}$$

Observed in Ross Sea by
F. Montiel, T. Milne,
A. Kohout and L. Roach
Presented at KOZWaves 2020

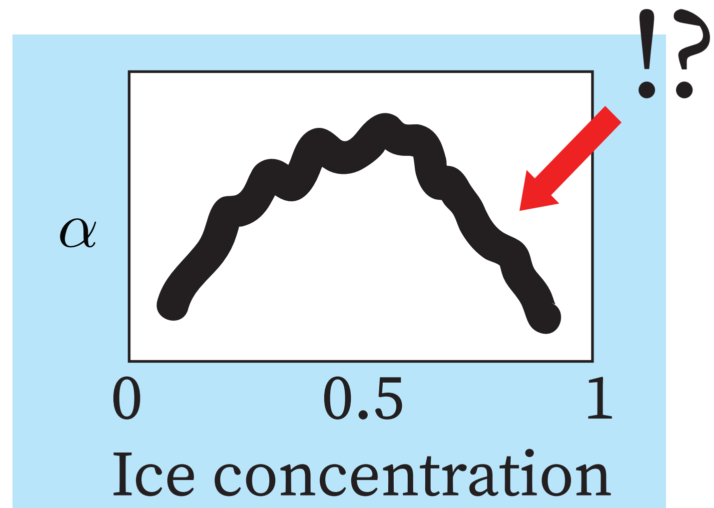

If ice concentration is high, randomly placed floes collide ✶ in groups of three or more.

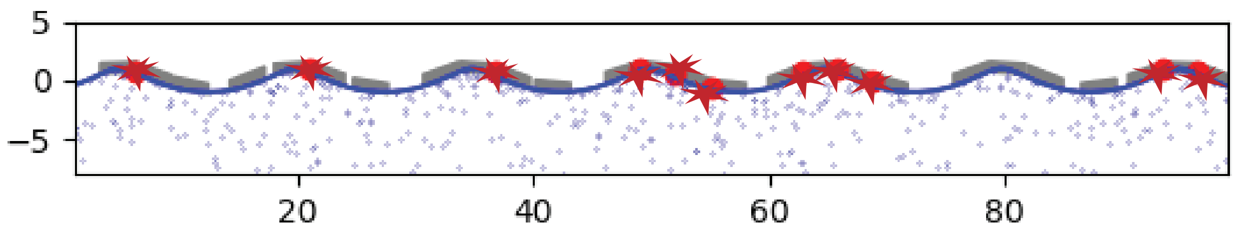

Floe spacing becomes more uniform and pairwise collisions predominate.

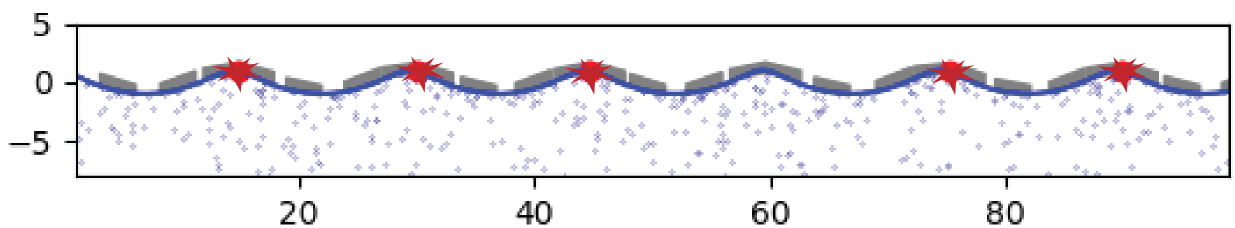

Simulate

- Airy waves
- Form drag
- Ice floe collisions

advection enhanced diffusion

effective diffusivity

nutrient and salt transport in sea ice
heat transport in sea ice with convection
sea ice floes in winds and ocean currents
tracers, buoys diffusing in ocean eddies
diffusion of pollutants in atmosphere

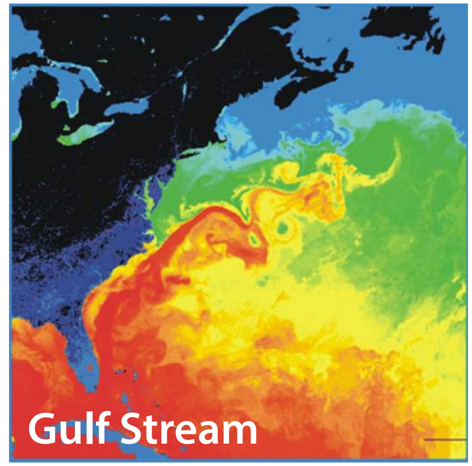

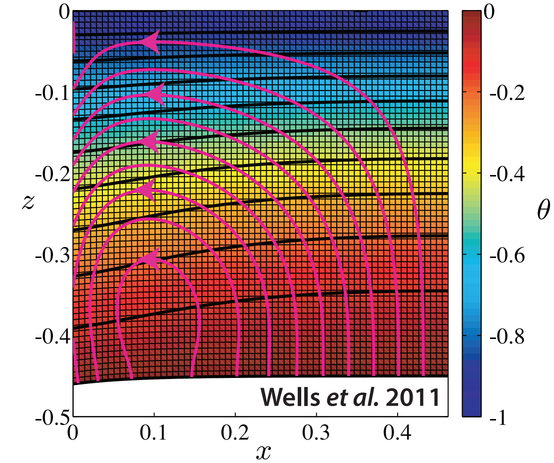

advection diffusion equation with a velocity field $\vec{u}$

$$\frac{\partial T}{\partial t} + \vec{u} \cdot \vec{\nabla} T = \kappa \Delta T$$

$$\vec{\nabla} \cdot \vec{u} = 0$$

↓ ***homogenize***

$$\frac{\partial \overline{T}}{\partial t} = \kappa^* \Delta \overline{T}$$

κ^* ***effective diffusivity***

Stieltjes integral for κ^* with spectral measure

Avellaneda and Majda, PRL 89, CMP 91

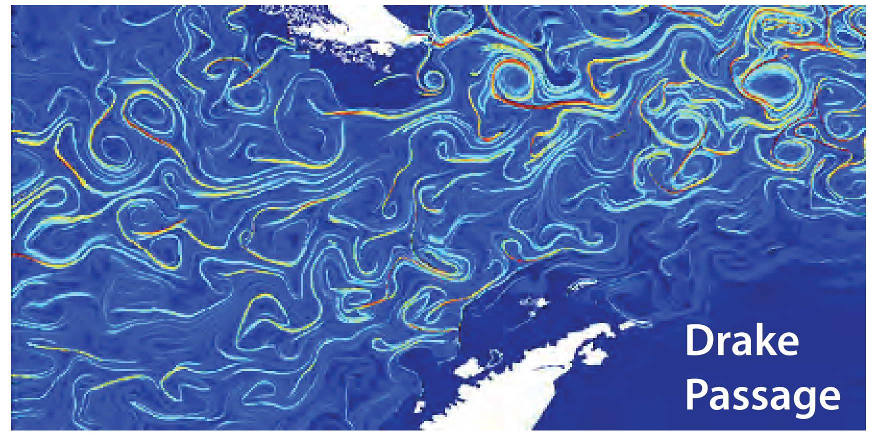

Murphy, Cherkaev, Xin, Zhu, Golden, *Ann. Math. Sci. Appl.* 2017
Murphy, Cherkaev, Zhu, Xin, Golden, *J. Math. Phys.* 2020

Stieltjes Integral Representation for Advection Diffusion

Murphy, Cherkaev, Zhu, Xin, Golden, *J. Math. Phys.* 2020

$$\kappa^* = \kappa \left(1 + \int_{-\infty}^{\infty} \frac{d\mu(\tau)}{\kappa^2 + \tau^2} \right), \quad F(\kappa) = \int_{-\infty}^{\infty} \frac{d\mu(\tau)}{\kappa^2 + \tau^2}$$

- μ is a positive definite measure corresponding to the spectral resolution of the self-adjoint operator $i\Gamma H \Gamma$
- $H =$ stream matrix , $\kappa =$ local diffusivity
- $\Gamma := -\nabla(-\Delta)^{-1}\nabla\cdot$, Δ is the Laplace operator
- $i\Gamma H \Gamma$ is bounded for time independent flows
- $F(\kappa)$ is analytic off the spectral interval in the κ-plane

rigorous framework for numerical computations of spectral measures and effective diffusivity for model flows

new integral representations, theory of moment calculations

separation of material properties and flow field

Rigorous bounds on convection enhanced thermal conductivity of sea ice

Kraitzman, Hardenbrook, Murphy, Zhu, Cherkaev, Strong, Golden 2020

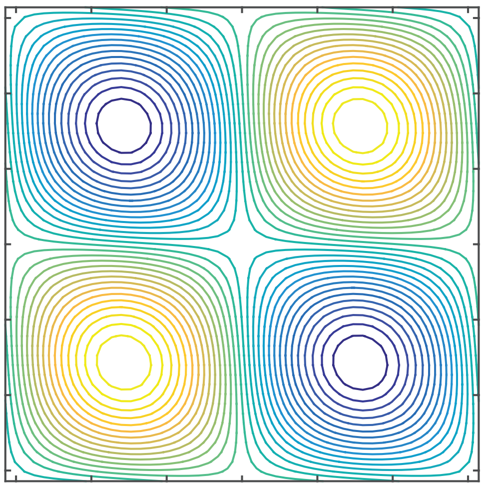

cat's eye flow model for brine convection cells

similar bounds
for shear flows

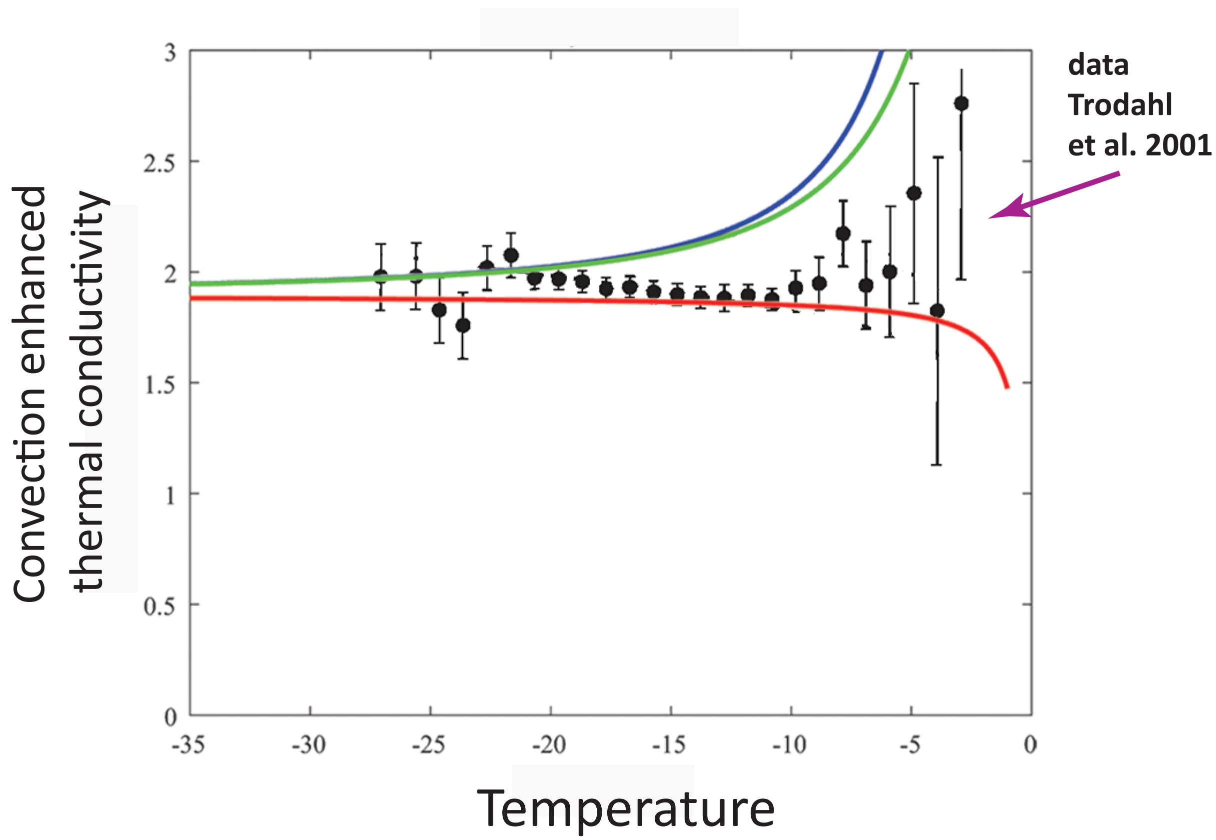

rigorous Padé bounds from Stieltjes integral +
analytical calculations of moments of measure

rigorous bounds assuming information on flow field INSIDE inclusions

Kraitzman, Cherkaev, Golden
***SIAM J. Appl. Math.* (in revision), 2020**

melt pond formation and albedo evolution:

- ***major drivers in polar climate***
- ***key challenge for global climate models***

numerical models of melt pond evolution, including topography, drainage (permeability), etc.

Lüthje, Feltham, Taylor, Worster 2006

Flocco, Feltham 2007

Skyllingstad, Paulson, Perovich 2009

Flocco, Feltham, Hunke 2012

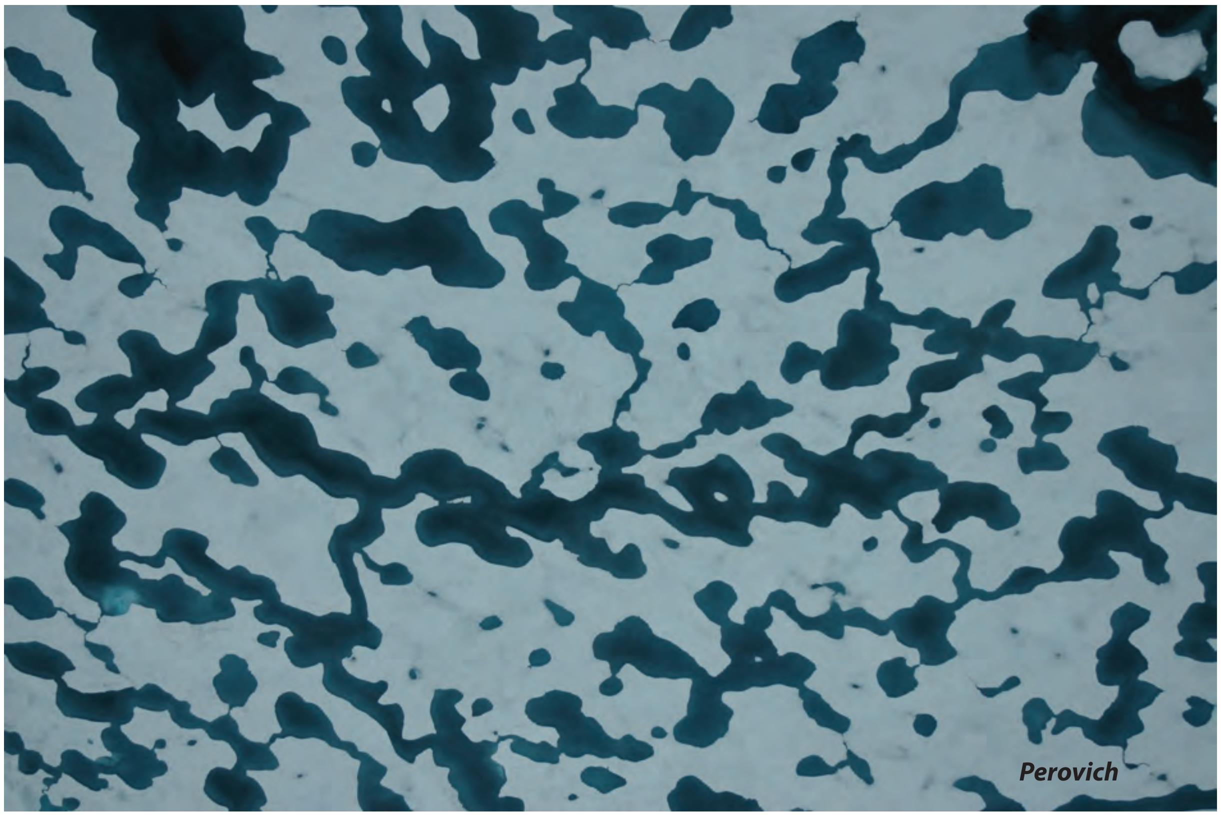

Are there universal features of the evolution similar to phase transitions in statistical physics?

Transition in the fractal geometry of Arctic melt ponds

Christel Hohenegger, Bacim Alali, Kyle Steffen, Don Perovich, Ken Golden

The Cryosphere, 2012

complexity grows with length scale

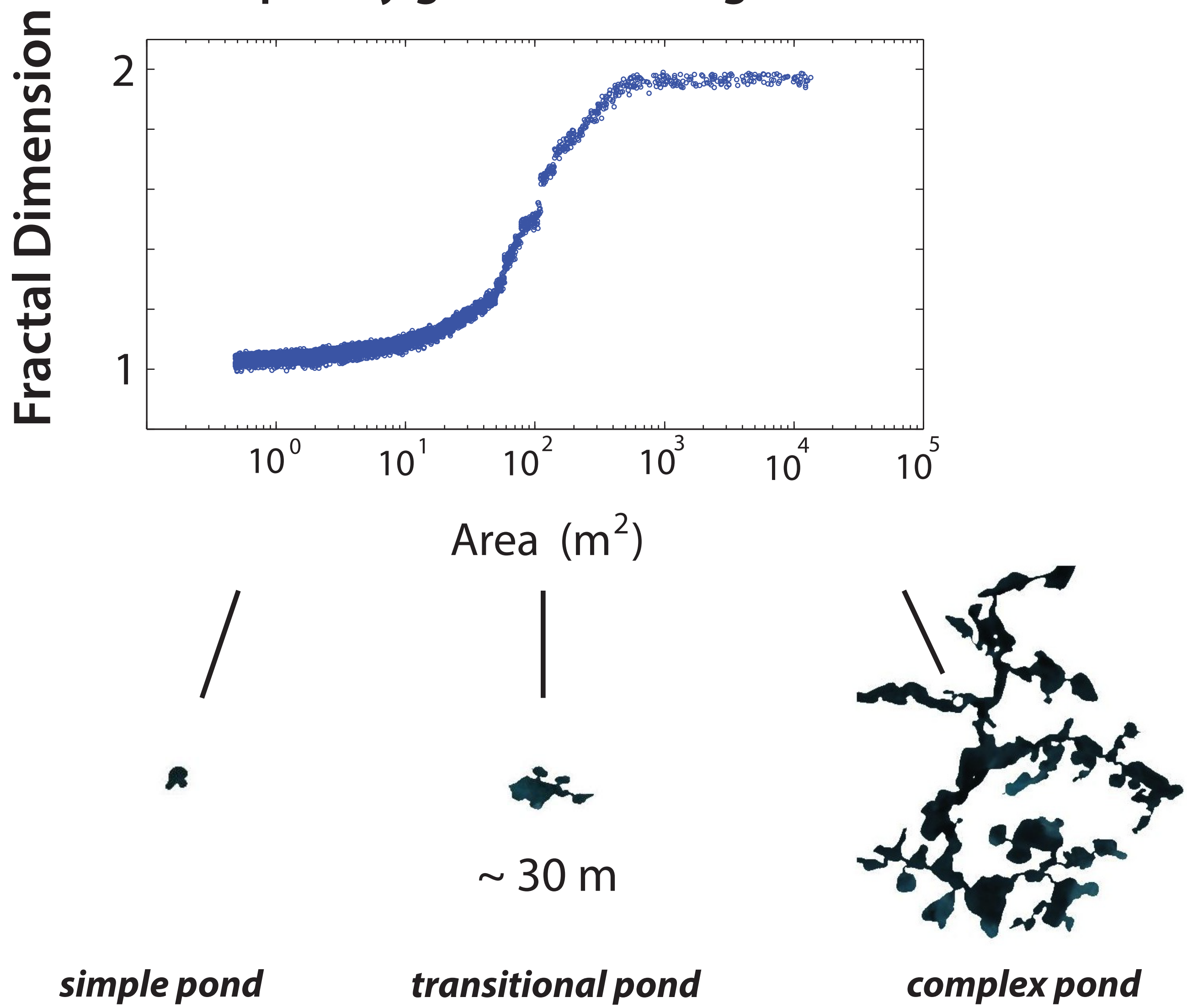

Continuum percolation model for melt pond evolution

level sets of random surfaces

Brady Bowen, Court Strong, Ken Golden, J. Fractal Geometry 2018

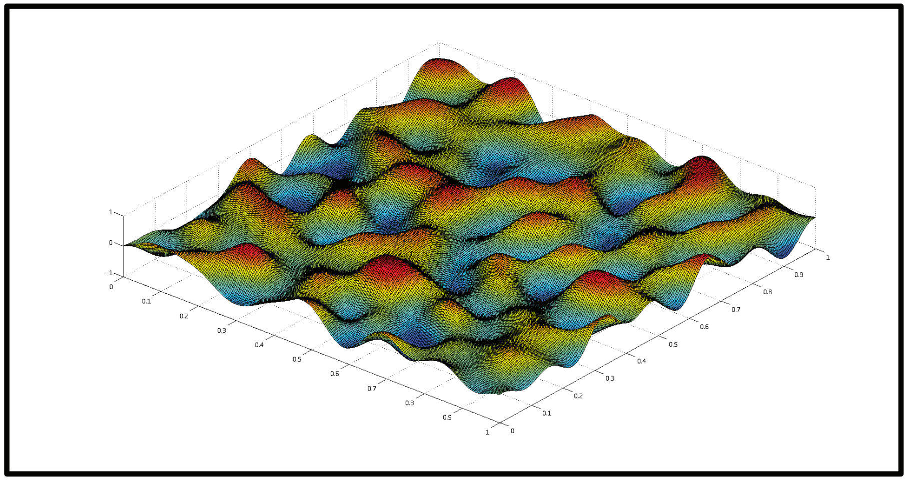

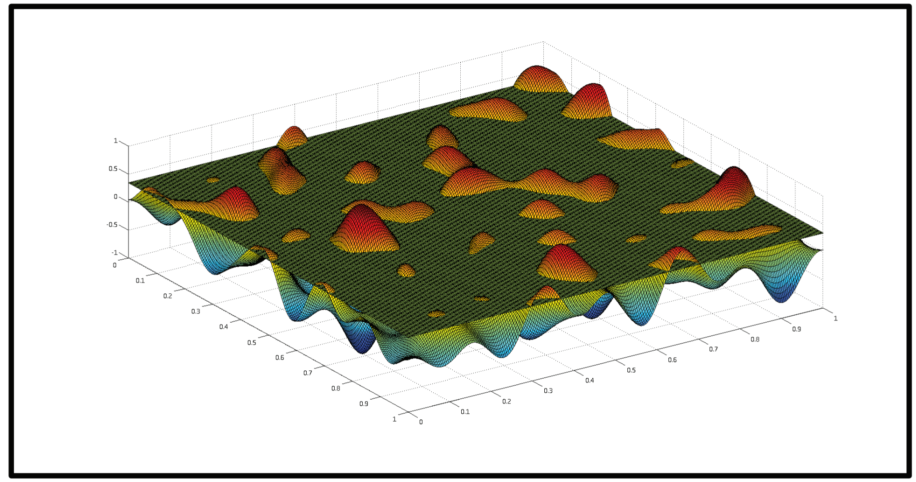

random Fourier series representation of surface topography

intersections of a plane with the surface deÿne melt ponds

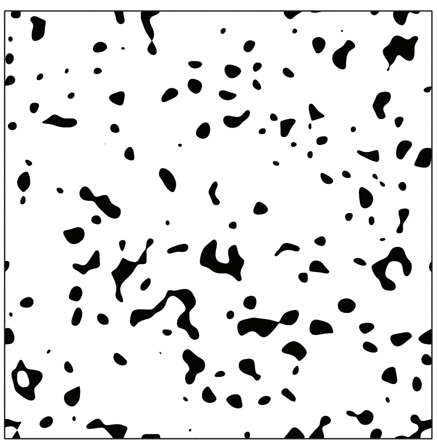

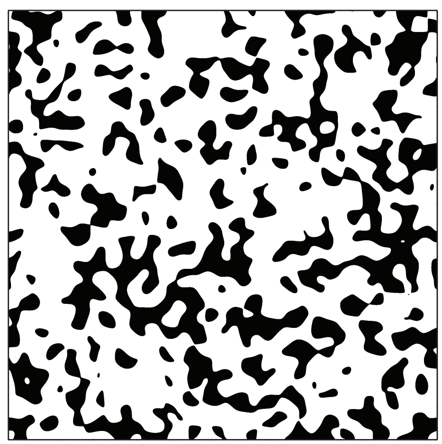

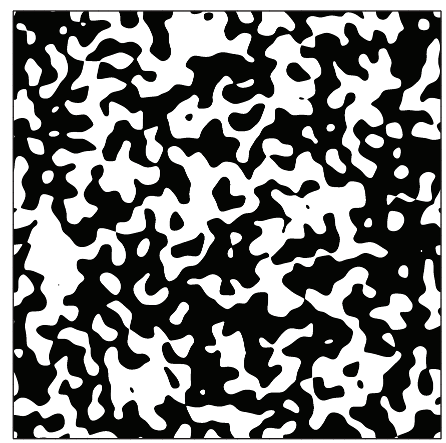

electronic transport in disordered media *diffusion in turbulent plasmas* *Isichenko, Rev. Mod. Phys., 1992*

fractal dimension curves depend on statistical parameters defining random surface

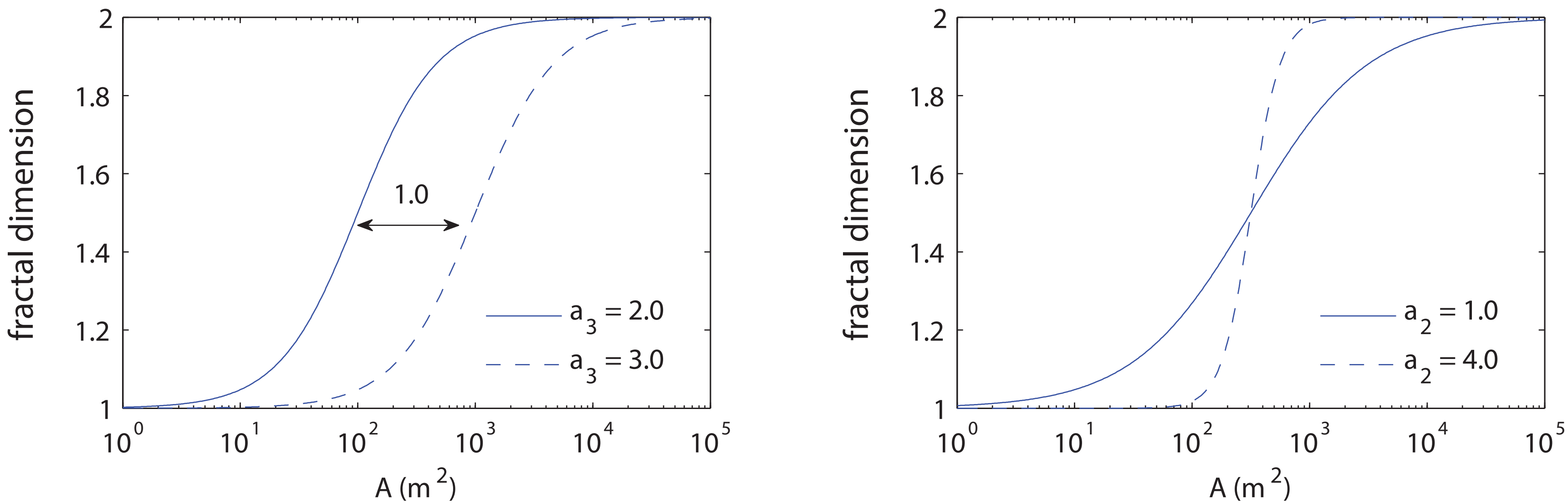

Saddle Points, Morse Theory and the Fractal Geometry of Melt Ponds

Ryleigh Moore, Jacob Jones, Dane Gollero, Court Strong, Ken Golden 2020

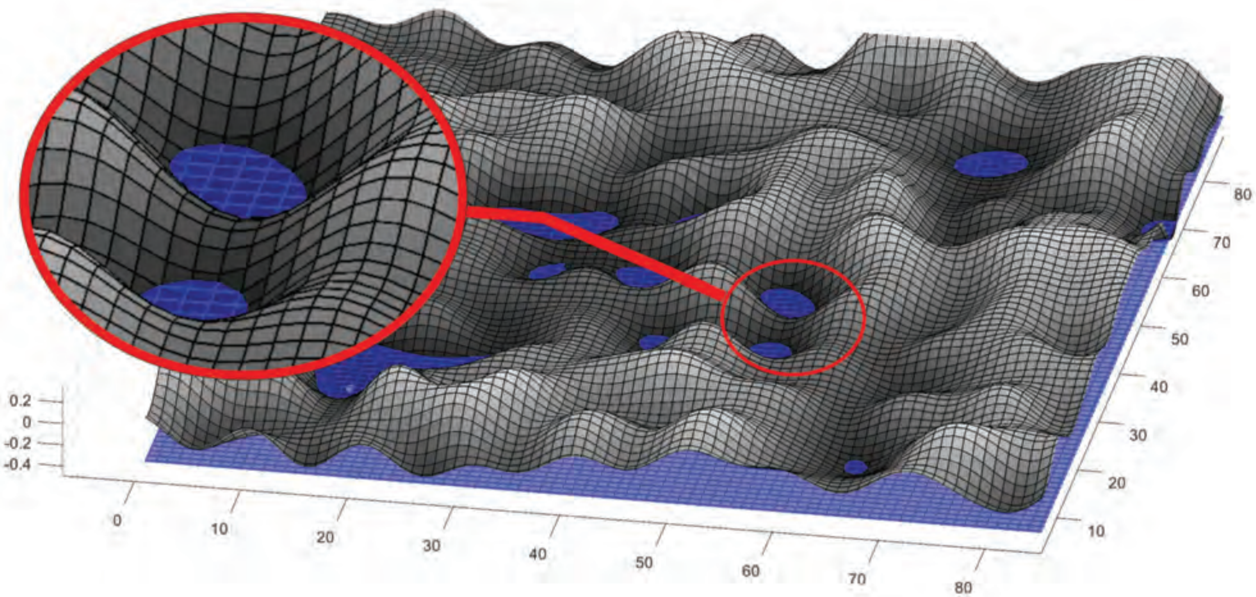

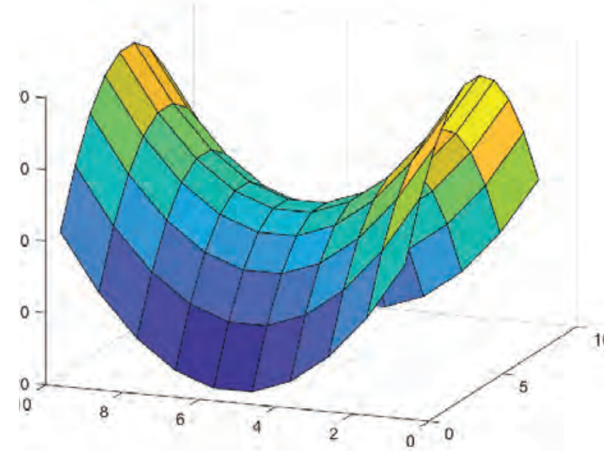

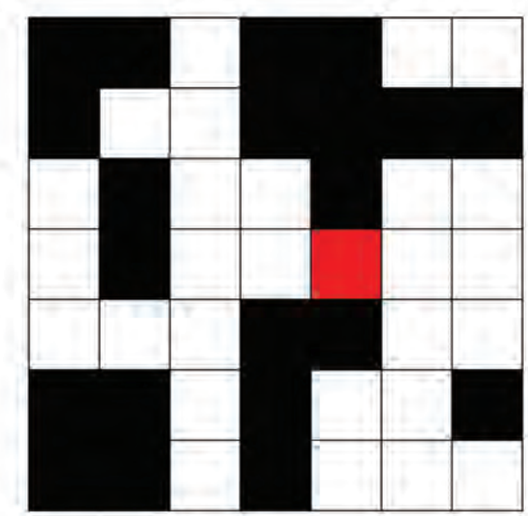

- Ponds connect through saddle points (Morse Theory).
- Red bond in lattice percolation theory ~ saddle point.

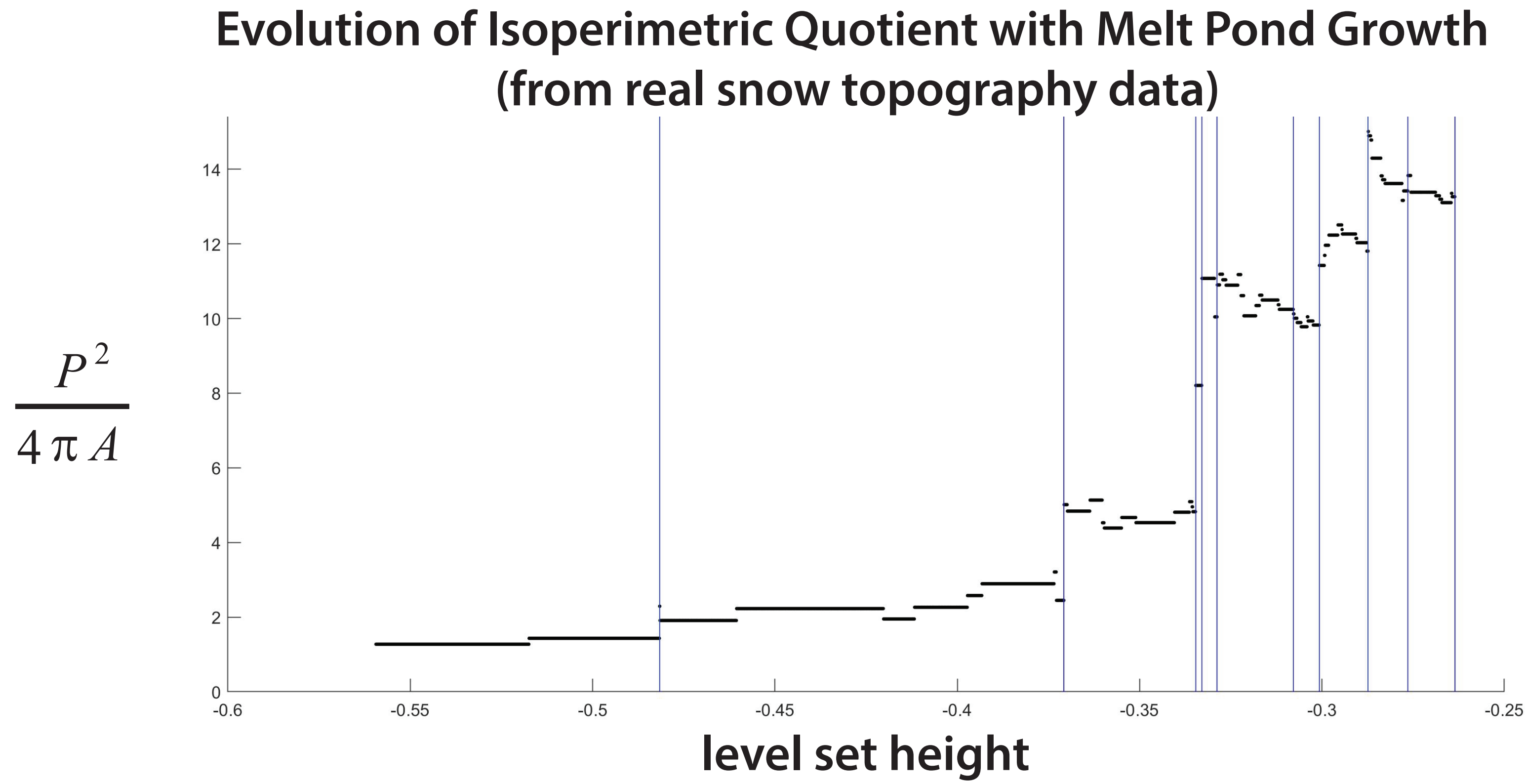

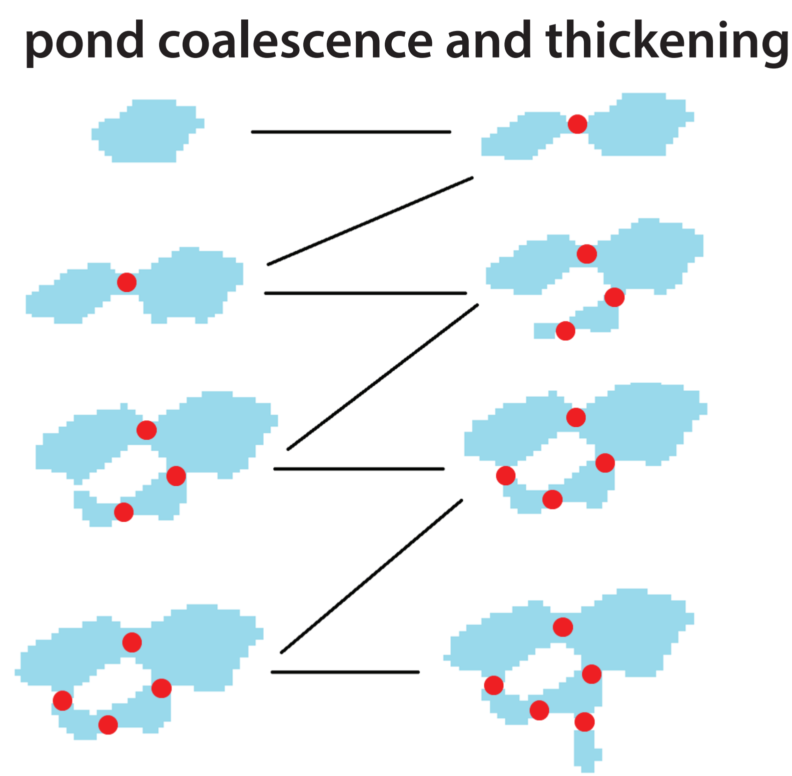

In the graph, we follow a single pond's growth. The vertical lines denote when the pond goes through a saddle point.

We see that large jumps in fractal dimension occur through saddle points.

Ryleigh Moore
Department of Mathematics
University of Utah

Multidisciplinary drifting Observatory for the Study of Arctic Climate (MOSAiC)

MOSAiC School
aboard the icebreaker ***RV Akademik Federov***

September 20 - October 28, 2019

20 grad students from around the world
(3 from U.S., 1 mathematician)

Ryleigh led successful installation of three seasonal ice mass balance (SIMB3) buoys in the Central Arctic.

Ising Model for a Ferromagnet

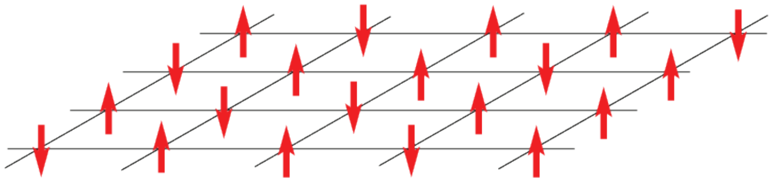

applied magnetic field $\uparrow H$

$$s_i = \begin{cases} +1 & \text{spin up} \\ -1 & \text{spin down} \end{cases}$$

blue

white

$$\mathcal{H} = -H \sum_i s_i - J \sum_{<i,j>} s_i s_j$$

nearest neighbor Ising Hamiltonian

ferromagnetic interaction $J \geq 0$

islands of like spins

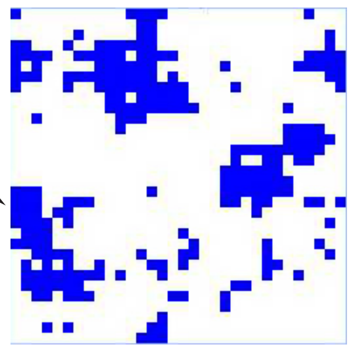

magnetization

homogenized parameter like effective conductivity

$$M(T,H) = \lim_{N \to \infty} \frac{1}{N} \left\langle \sum_j s_j \right\rangle$$

energy is lowered when nearby spins align with each other, forming magnetic domains

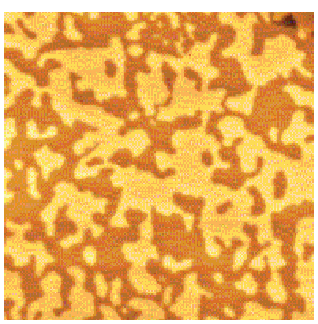

magnetic domains in cobalt

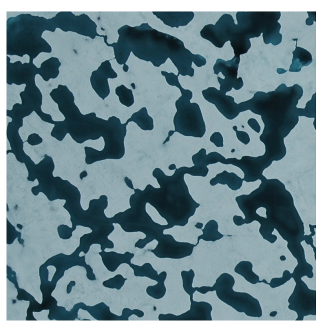

melt ponds (Perovich)

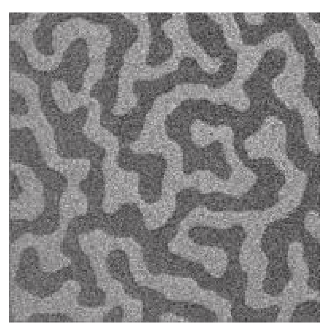

magnetic domains in cobalt-iron-boron

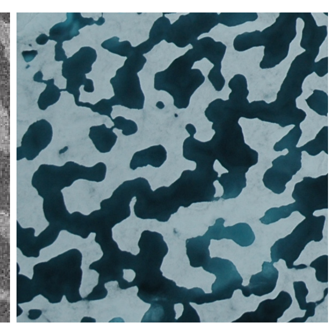

melt ponds (Perovich)

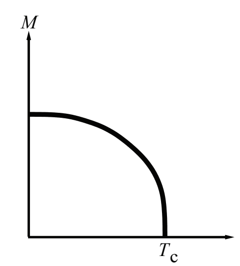

Curie point critical temperature

Ising model for ferromagnets ⟶ Ising model for melt ponds

Ma, Sudakov, Strong, Golden, *New J. Phys.*, 2019

$$\mathcal{H} = -\sum_{i}^{N} H_i\, s_i - J \sum_{<i,j>}^{N} s_i s_j \qquad s_i = \begin{cases} \uparrow \quad +1 \quad \text{water} \quad \text{(spin up)} \\ \downarrow \quad -1 \quad \text{ice} \quad \text{(spin down)} \end{cases}$$

random magnetic field represents snow topography

magnetization M

pond area fraction *~ albedo*

$$F = \frac{(M+1)}{2}$$

only nearest neighbor patches interact

Starting with random initial configurations, as Hamiltonian energy is minimized by Glauber spin flip dynamics, system "flows" toward metastable equilibria.

Order from Disorder

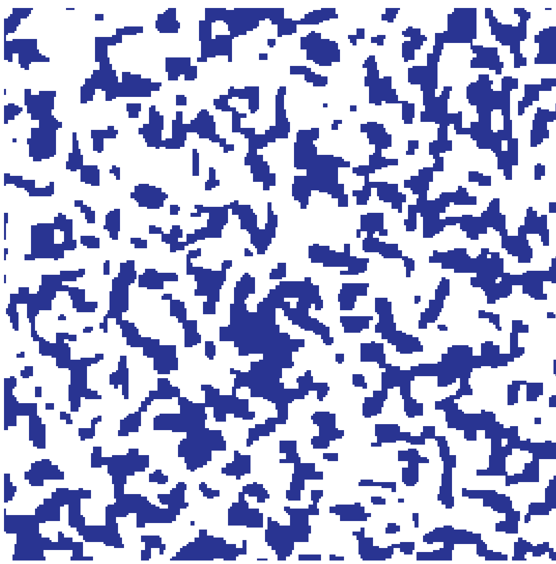

Ising model

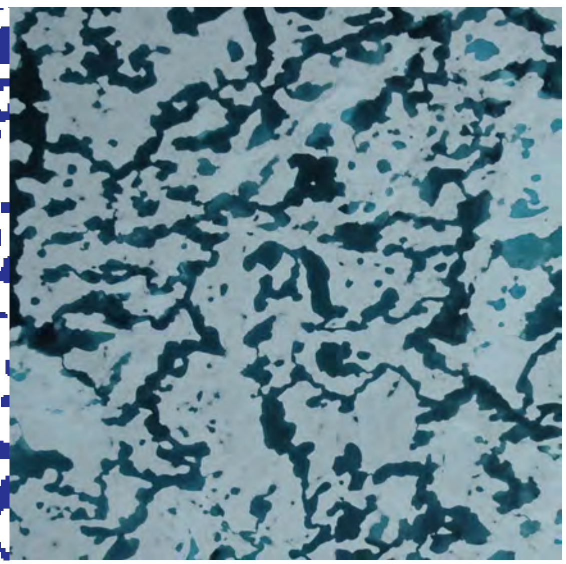

melt pond photo (Perovich)

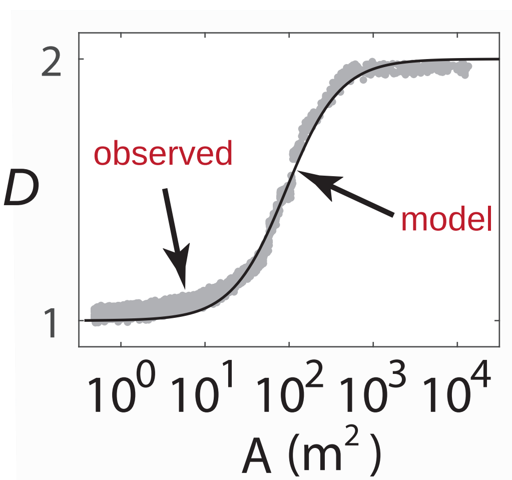

pond size distribution exponent

observed -1.5

(Perovich, *et al.* 2002)

model -1.58

Scientific American
EOS, PhysicsWorld, ...

ONLY MEASURED INPUT = LENGTH SCALE (GRID SIZE) from snow topography data

The effect of melt pond geometry on the distribution of solar energy under first-year sea ice

Horvat, Flocco, Rees Jones, Roach, Golden, *Geophys. Res. Lett.* 2020

- Model for 3D light field under ponded sea ice.
- Distribution of solar energy at depth influenced by ***shape and connectivity*** of melt ponds, as well as area fraction.
- Aggregate properties of the sub-ice light field, such as a significant enhancement of available solar energy under the ice, are controlled by parameter closely related to pond fractal geometry.
- Model and analysis explain how melt pond geometry ***homogenizes*** under-ice light field, affecting habitability.

Pond geometry affects ecology and partitioning of solar energy in the upper Arctic Ocean.

2011 massive under-ice algal bloom

Arrigo et al., *Science* 2012

melt ponds act as

WINDOWS

allowing light through sea ice

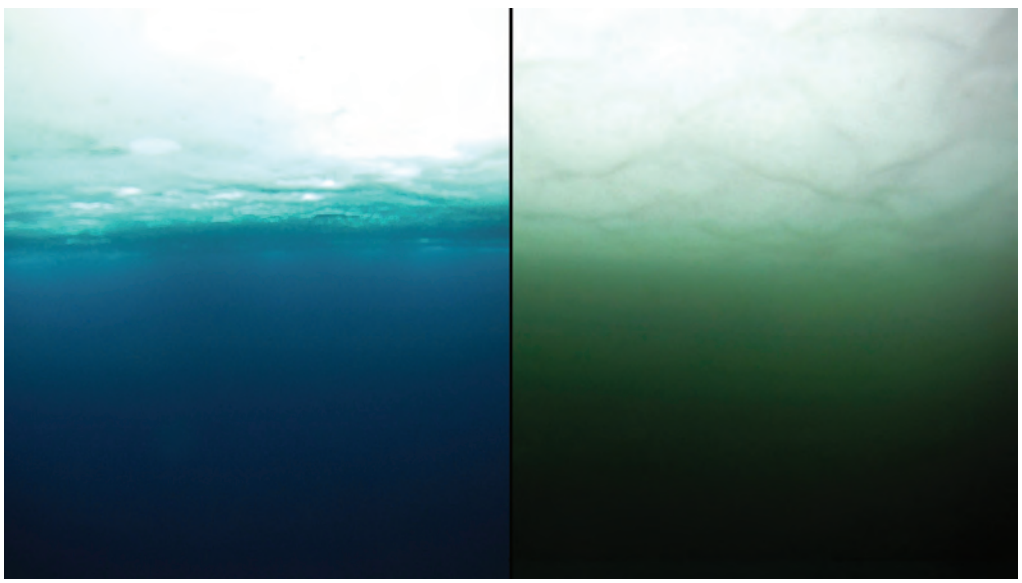

no bloom

bloom

Have we crossed into a new ecological regime?

The frequency and extent of sub-ice phytoplankton blooms in the Arctic Ocean

Horvat, Rees Jones, Iams, Schroeder, Flocco, Feltham, *Science Advances*, 2017

(2015 AMS MRC, Snowbird)

macroscale

Anomalous diffusion in sea ice dynamics

Ice floe diffusion in winds and currents

Jennifer Lukovich, Jennifer Hutchings, David Barber, *Ann. Glac.* 2015

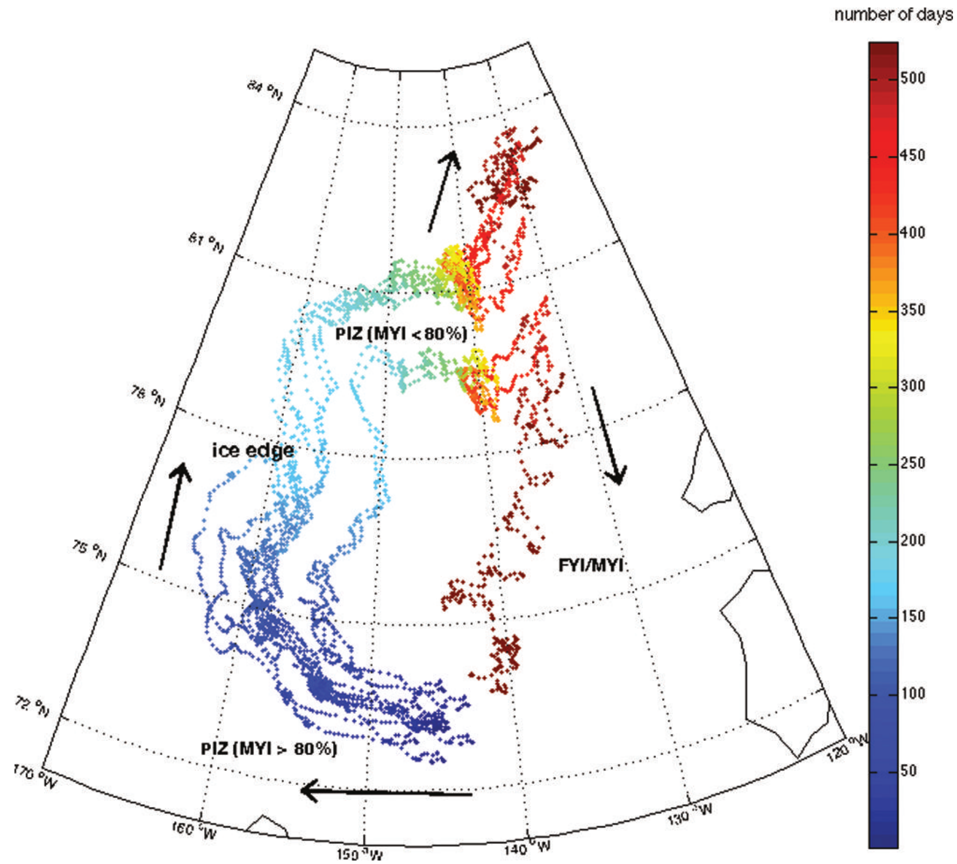

- On short time scales floes observed (buoy data) to exhibit Brownian-like behavior, but they are also being advected by winds and currents.

- Effective behavior is purely diffusive, sub-diffusive or super-diffusive depending on ice pack and advective conditions - Hurst exponent.

Floe Scale Model of Anomalous Diffusion in Sea Ice Dynamics

Huy Dinh, Elena Cherkaev, Court Strong, Ken Golden 2019

$$\left\langle \left| \mathbf{x}(t) - \mathbf{x}(0) - \langle \mathbf{x}(t) - \mathbf{x}(0) \rangle \right|^2 \right\rangle \sim t^{\alpha}$$

$\alpha =$ Hurst exponent, a measure of anomalous diffusion.

Measured from bouy position data. Detects ice pack crowding and advective forcing.

J.V. Lukovich, J.K. Hutchings, D.G. Barber ***Annals of Glaciology*** **2015**

diffusive $\alpha = 1$ Sparse packing, uncorrelated advective field.

sub-diffusive $\alpha < 1$ Dense packing, crowding dominates advection.

super-diffusive $\alpha = 5/4$ Sparse packing, shear dominates advection.

$\alpha = 5/3$ Sparse packing, vorticity dominates advection.

Goal: Develop numerical model to analyze regimes of transport in terms of ice pack crowding and advective conditions.

Model Results

Crowding in random advective forcing.

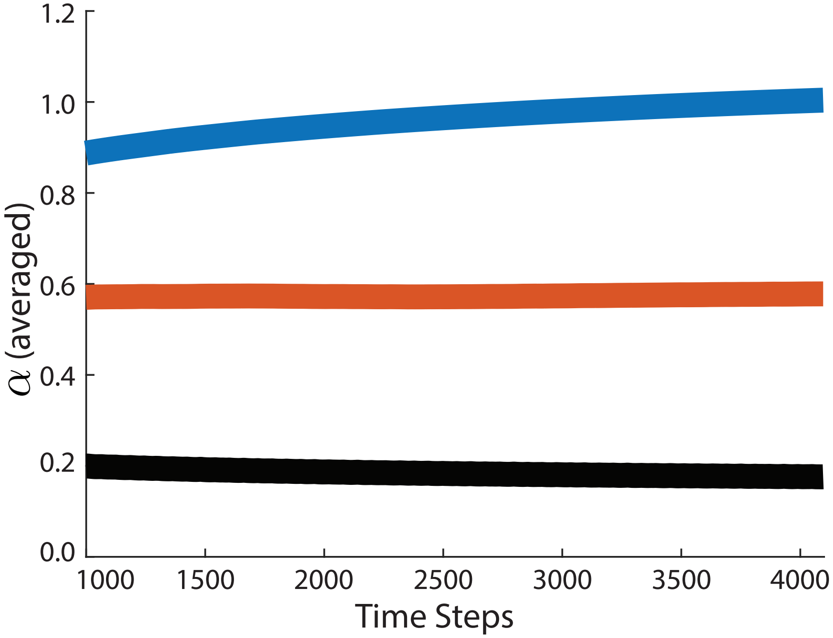

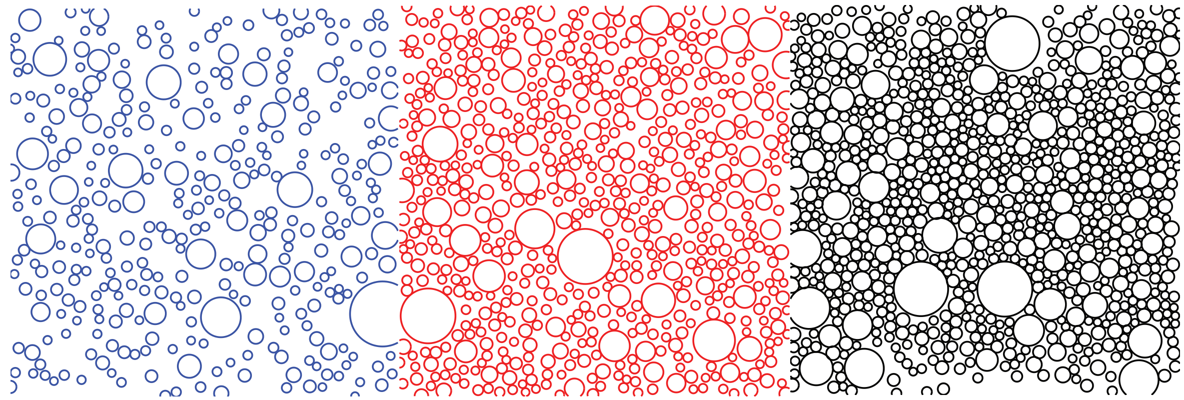

Concentration = 0.3 k = 2.9

Concentration = 0.5 k = 2.9

Concentration = 0.7 k = 2.9

Concentration = 0.3 k = 2.9

Vorticity Dominated Drift

$\alpha = 5/3$

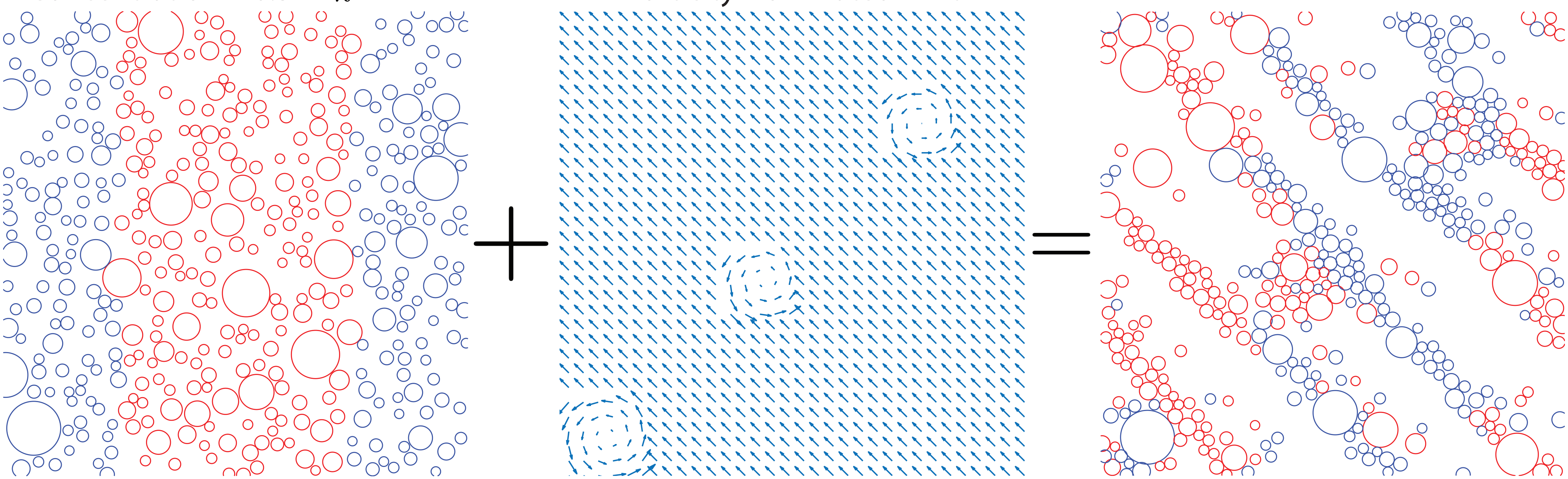

Marginal Ice Zone

MIZ

- biologically active region
- intense ocean-sea ice-atmosphere interactions
- region of significant wave-ice interactions

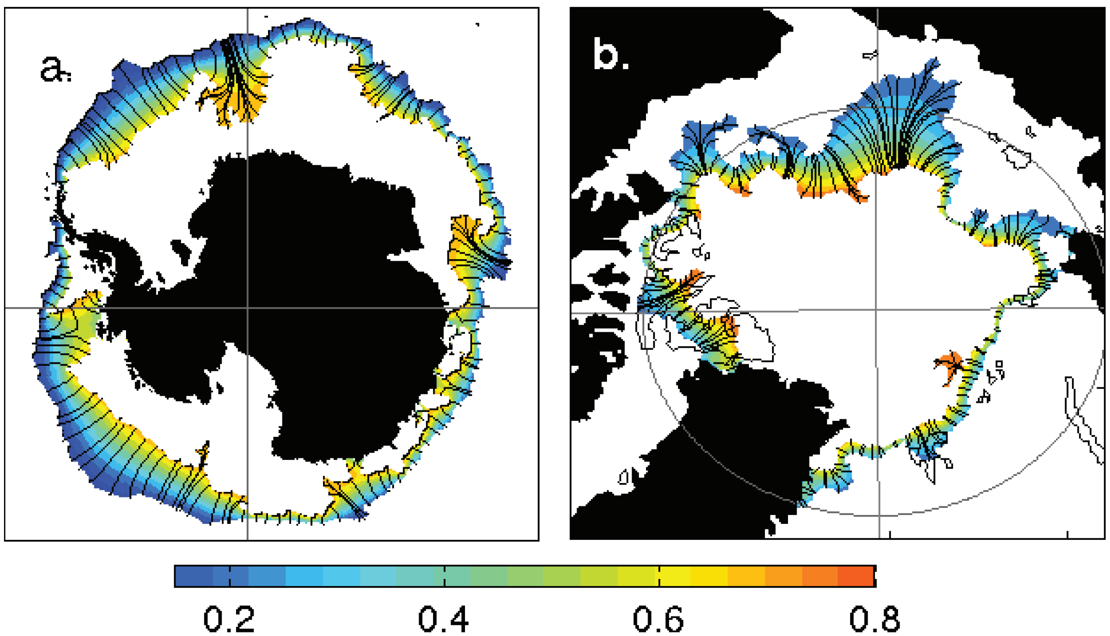

transitional region between dense interior pack ($c > 80\%$) sparse outer fringes ($c < 15\%$)

MIZ WIDTH
fundamental length scale of ecological and climate dynamics

Strong, *Climate Dynamics* 2012
Strong and Rigor, *GRL* 2013

How to objectively measure the "width" of this complex, non-convex region?

Objective method for measuring MIZ width motivated by medical imaging and diagnostics

Strong, *Climate Dynamics* 2012
Strong and Rigor, *GRL* 2013

39% widening
1979 - 2012

streamlines of a solution to Laplace's equation

"average" lengths of streamlines

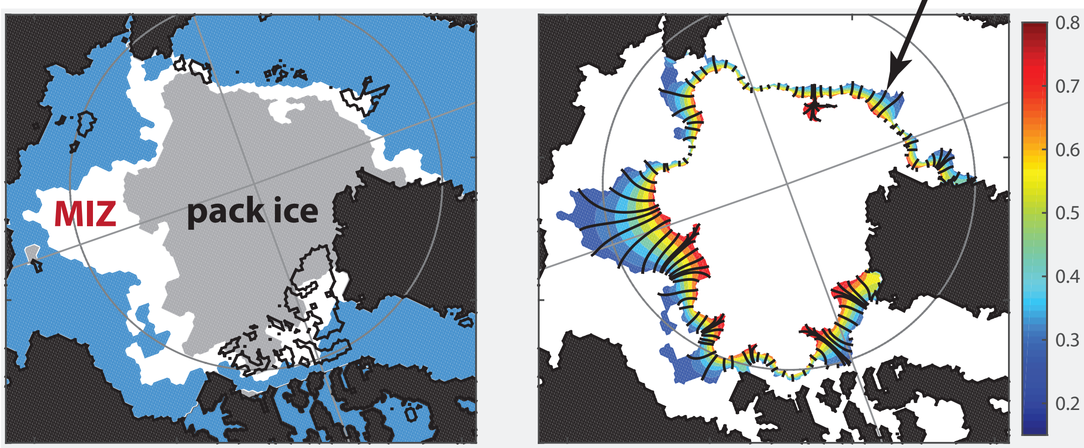

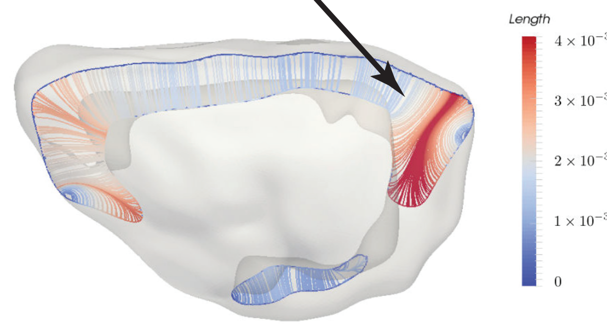

Arctic Marginal Ice Zone

crossection of the cerebral cortex of a rodent brain

analysis of different MIZ WIDTH definitions

Strong, Foster, Cherkaev, Eisenman, Golden
J. Atmos. Oceanic Tech. 2017

Strong and Golden
Society for Industrial and Applied Mathematics News, April 2017

Filling the polar data gap

hole in satellite coverage
of sea ice concentration ÿeld

previously assumed ice covered

Gap radius: 611 km
06 January 1985

Gap radius: 311 km
30 August 2007

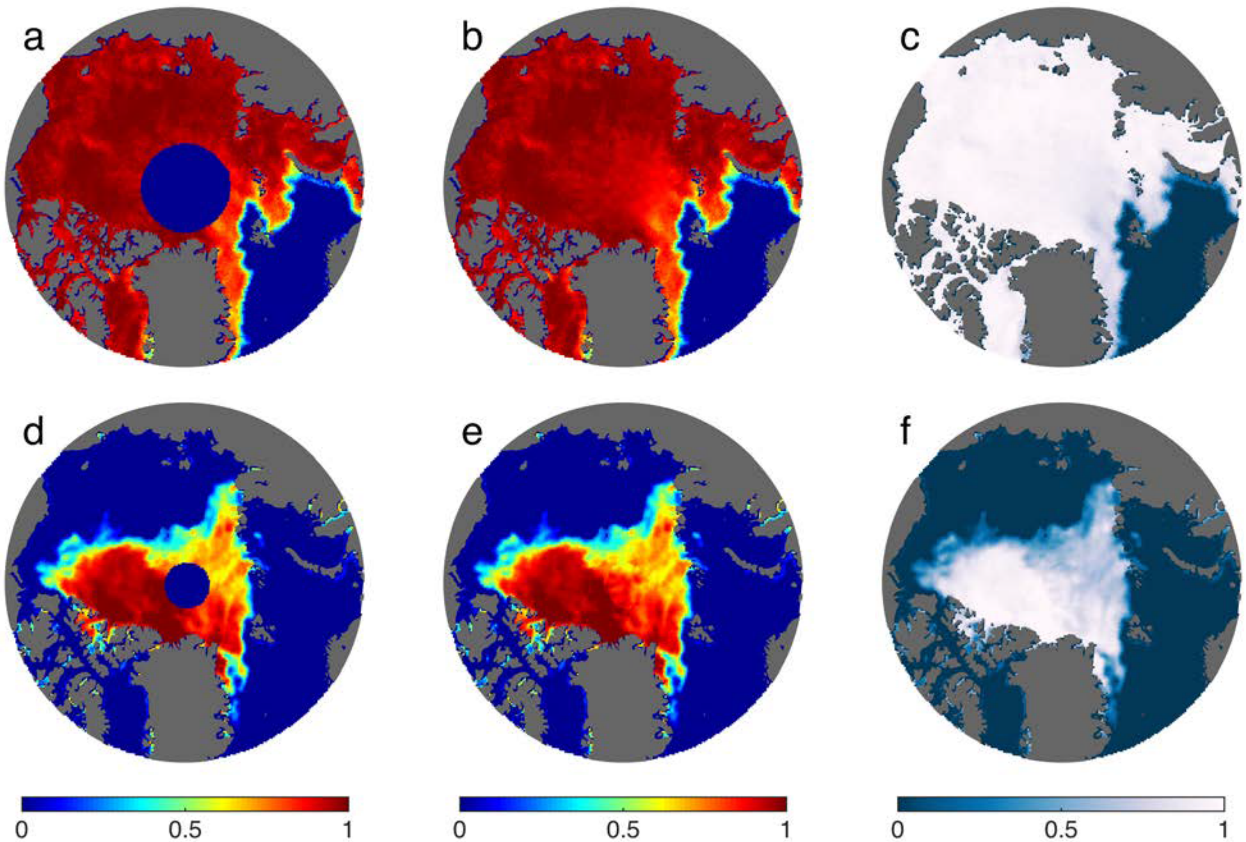

fill with harmonic function satisfying
satellite BC's plus stochastic term

Strong and Golden, *Remote Sensing* 2016
Strong and Golden, *SIAM News* 2017

Conclusions

1. Sea ice is a fascinating multiscale composite with structure similar to many other natural and man-made materials.

2. Mathematical methods developed for sea ice advance the theory of composites and inverse problems in general.

2. Homogenization and statistical physics help ***link scales in sea ice and composites***; provide rigorous methods for finding effective behavior; advance sea ice representations in climate models.

3. Fluid flow through sea ice mediates melt pond evolution and many processes important to climate change and polar ecosystems.

5. Field experiments are essential to developing relevant mathematics.

6. Our research will help to improve projections of climate change, the fate of Earth's sea ice packs, and the ecosystems they support.

Buchanan Bay, Antarctica   Mertz Glacier Polynya Experiment   July 1999

Two Layer Models and Effective Rheological Parameters

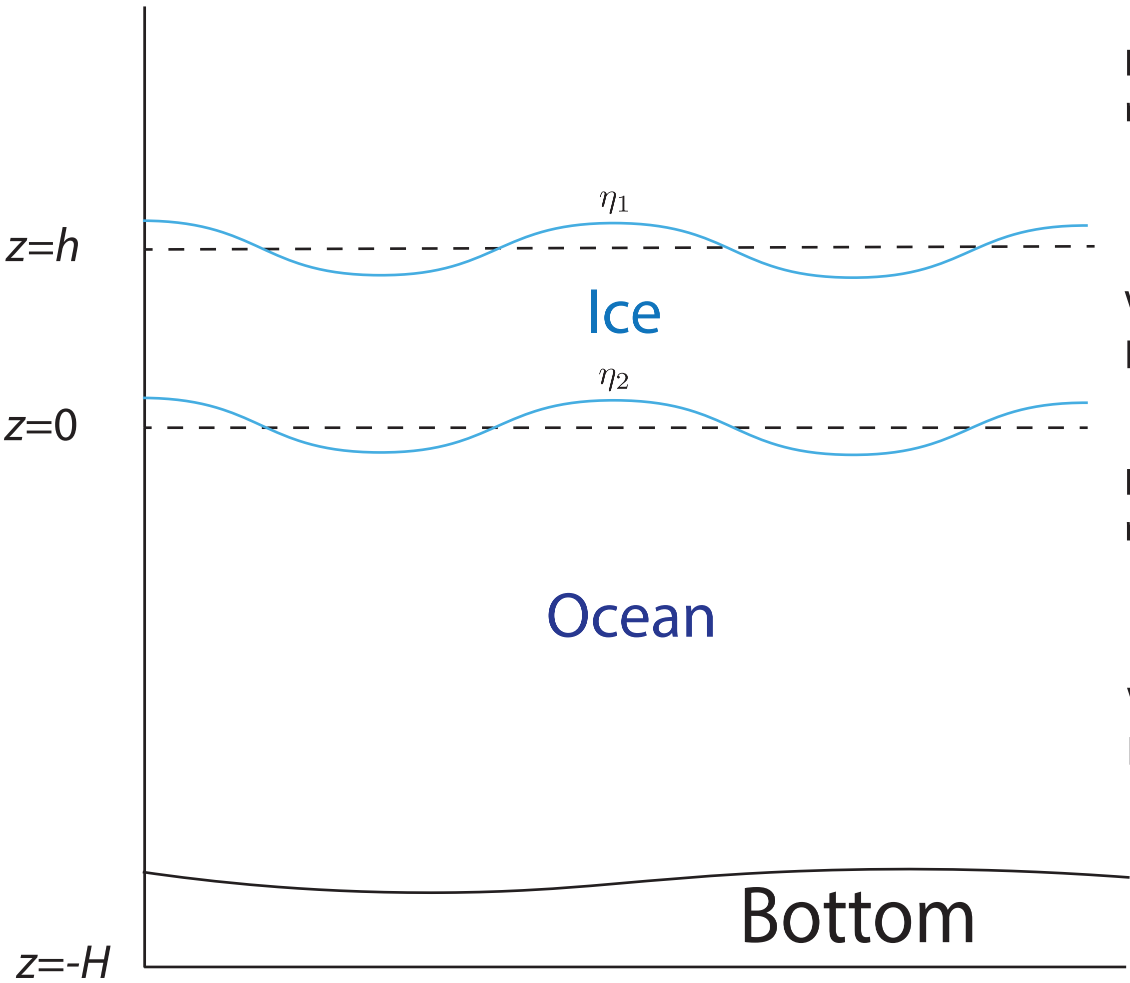

G shear modulus P pressure ω angular frequency U velocity field

ν viscosity λ Poission ratio ρ density g gravity

Viscous fluid layer (Keller 1998)
E˜ ective Viscosity $\boxed{\nu}$

Equations of motion: $$\frac{\partial U}{\partial t} = -\frac{1}{\rho}\nabla P + \nu \nabla^2 U + g$$

Viscoelastic fluid layer (Wang-Shen 2010)
E˜ ective Complex Viscosity $\boxed{\nu_e = \nu + iG/\rho\omega}$

Equations of motion $$\frac{\partial U}{\partial t} = -\frac{1}{\rho}\nabla P + \nu_e \nabla^2 U + g$$

Viscoelastic thin beam (Mosig *et al.* 2015)
E˜ ective Complex Shear Modulus $\boxed{G_v = G - i\omega\rho\nu}$

Stieltjes integral representation for effective complex viscoelastic parameter; bounds

Sampson, Murphy, Cherkaev, Golden 2019

Homogenization for two phase viscoelastic composite

$$\nu_1 = 10^7 + i\,4875$$ **pancake ice**

$$\nu_2 = 5 + i\,0.0975$$ **slush / frazil**

microscale $$\sigma = C_{ijkl}\epsilon_{kl} = C:\epsilon$$

$$C = 2(\chi_1\nu_1 + \chi_2\nu_2)\Lambda_s$$

macroscale $$\langle\sigma\rangle = C^*:\langle\epsilon\rangle$$

$$\langle\epsilon\rangle = \epsilon^0$$

quasistatic assumption $$\nabla\cdot\sigma = 0$$

Strain Field

$$\epsilon = \frac{1}{2}[\nabla u + (\nabla u)^T] = \nabla^s u \quad \nabla\cdot u = 0$$

Resolvent

$$\epsilon = \left(1 - \frac{1}{s}\Gamma\chi_1\right)^{-1}\epsilon^0 \Rightarrow \boxed{\frac{\nu^*}{\nu_2} = \left(1 - ||\epsilon^0||^{-2}F(s)\right)}$$

$$F(s) = \int_0^1 \frac{d\mu(\lambda)}{s-\lambda} \qquad s = \frac{1}{1-\frac{\nu_1}{\nu_2}}$$

$$\Gamma = \nabla^s(\nabla\cdot\nabla^s)^{-1}\nabla\,\cdot$$

Model Approximations

Floes $\approx$ Discs

Forces on Disc $= \quad F_{drag} + F_{collision}$

A. Herman ***Physical Review E*** **2011**

Floe-Floe Interactions: Linear Elastic Collisions

$F_{collision}$ follows Hooke's Law.

Advective Forcing: Passive, Linear Drag Law

v is the advective velocity field.

F_{drag} is proportional to relative velocity.

Ice Pack Characteristics

ϕ = sea ice concentration (floe area fraction)

Power Law Size Distribution: $N(D) \sim D^{-k}$

T. Toyota, S. Takatsuji, M. Nakayama Geophysical Review Letters 2006

k = floe diameter exponent

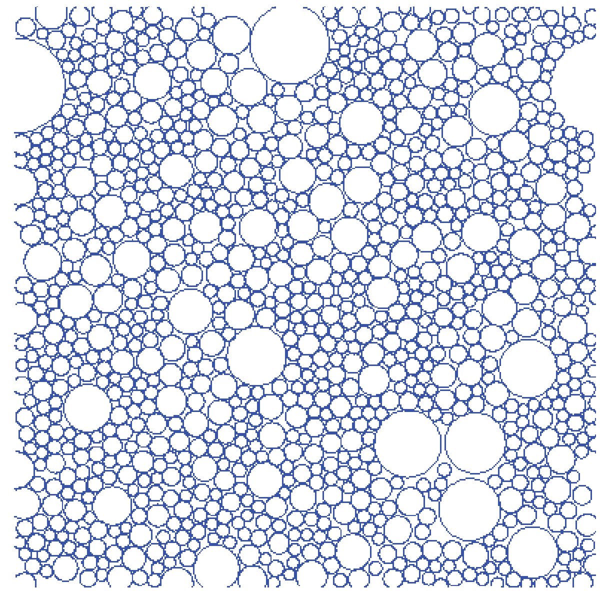

$k = 2.9$, $\phi = 0.8$

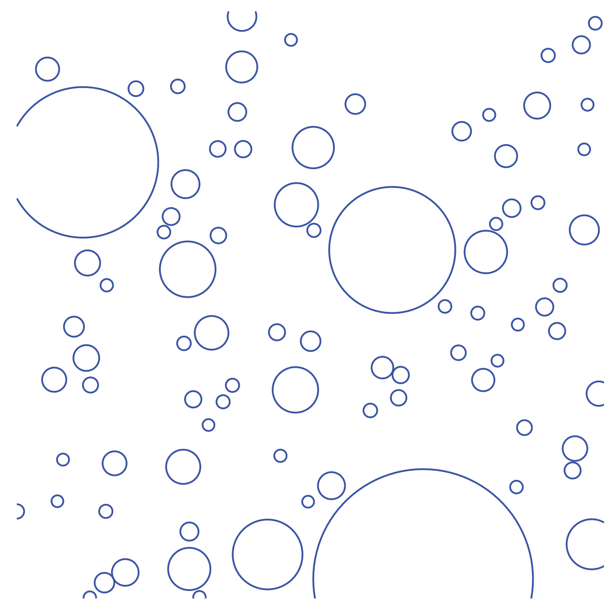

$k = 1.7$, $\phi = 0.1$

Model Results

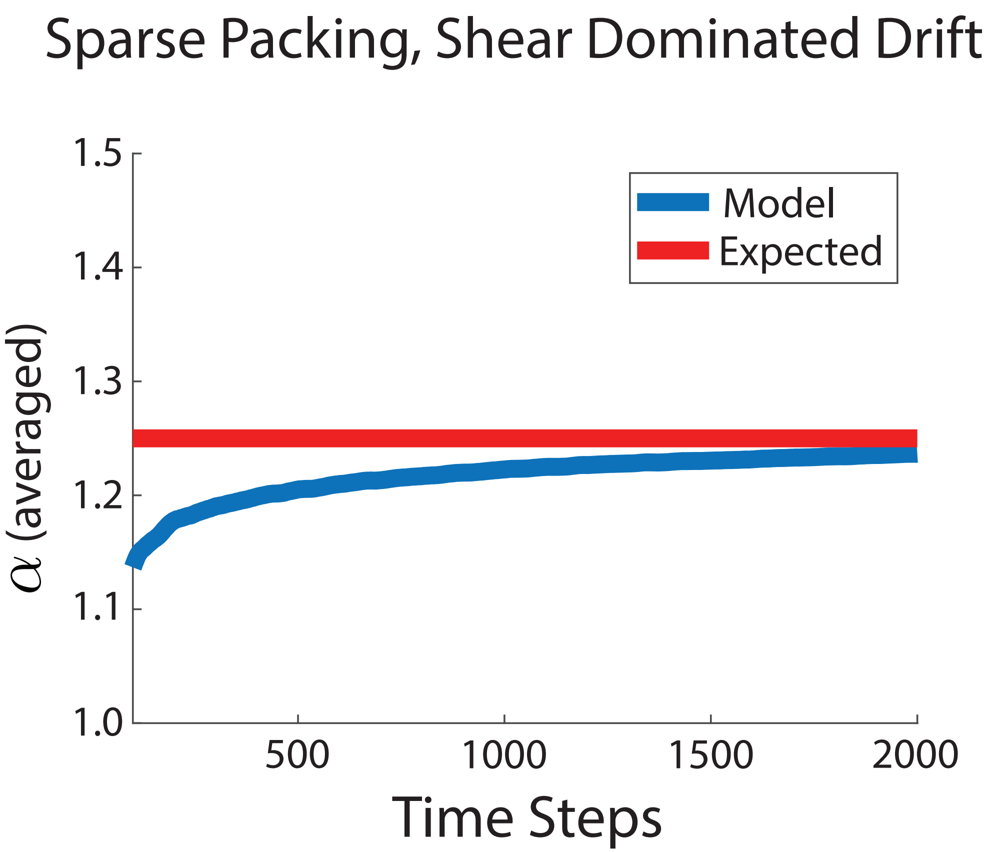

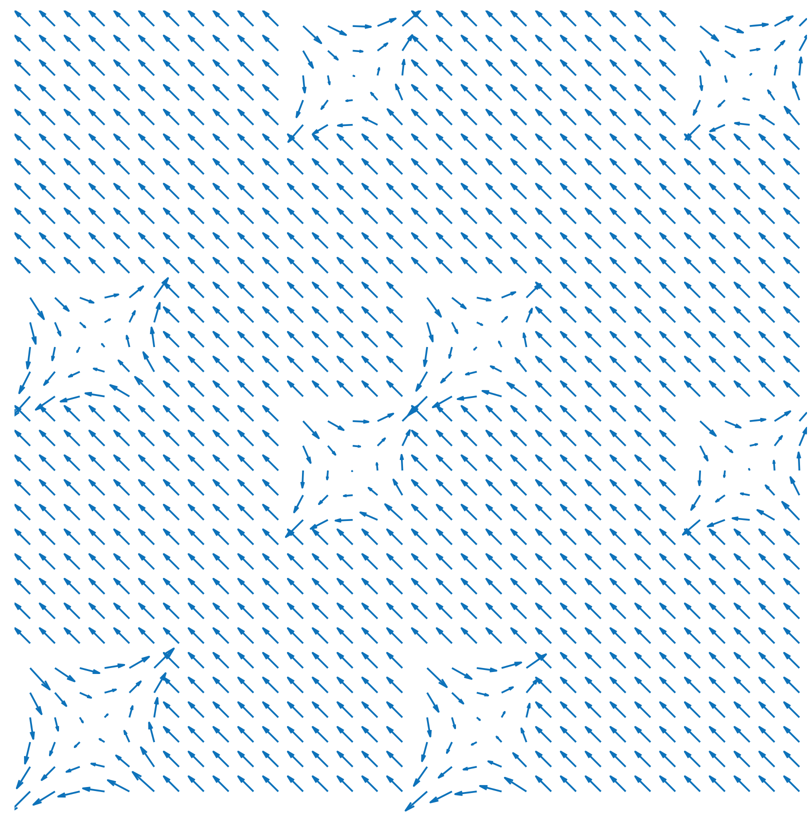

Expected $\alpha = 5/4$

k = 2.9 Concentration = 0.3

photo by Jan Lieser

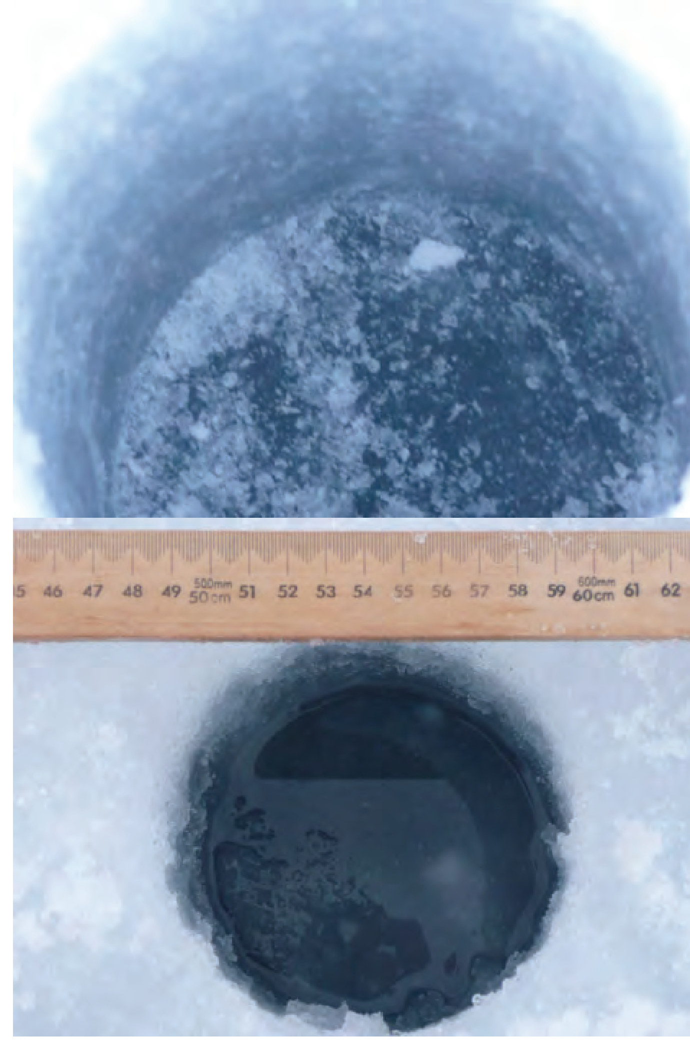

measuring fluid permeability of Antarctic sea ice

SIPEX 2007